EXAMINING THE EFFECTS OF FOLLISTATIN ON VESSEL CONTRACTION

EXAMINING THE EFFECTS OF FOLLISTATIN ON CONTRACTION OF VESSELS FROM NORMOTENSIVE AND HYPERTENSIVE RATS

NIKI SADAT AFJEH, BSc.

A Thesis Submitted to the Graduate Studies in Partial Fulfilment of the Requirements for the Degree Master of Medical Sciences

McMaster University

© Copyright by Niki Sadat Afjeh, June 2024

MASTER OF SCIENCE McMaster University

Medicine (Division of Nephrology) Hamilton, Ontario

TITLE: Examining the Effects of Follistatin on Contraction of Vessels from Normotensive and Hypertensive Rats

AUTHOR: Niki Sadat Afjeh, Honours BSc. (McMaster University)

SUPERVISORS: Dr. Joan Krepinsky and Dr. Jeffrey Dickhout

NUMBER OF PAGES: 99

LAY ABSTRACT

We had shown that a protein called follistatin can reduce high blood pressure in rats. High blood pressure, or hypertension, is a condition that can lead to health problems such as heart failure, kidney disease and death, if not managed properly. We focused on a type of rat called the Spontaneously Hypertensive Rat (SHR), which has high blood pressure similar to what people experience. Our goal was to understand how follistatin works to lower blood pressure. To do this, we looked at how the blood vessels in these rats responded to a substance called potassium chloride (KCl), which causes blood vessels to contract as they do with high blood pressure. We found that follistatin reduced contraction of blood vessels caused by KCl. We also observed that calcium and potassium levels inside muscle cells of the blood vessels were lowered with follistatin, which could be one way follistatin prevents contraction and relaxes blood vessels. A better understanding of how drugs affect blood vessels will help us to create new treatments for high blood pressure.

ABSTRACT

We have previously shown that short-term treatment (30 minutes) with follistatin (FST), a glycoprotein inhibitor of activins, reduced contraction caused by potassium (KCl) in vessels of the Spontaneously Hypertensive Rat (SHR) model of essential hypertension. This study specifically investigates the mechanisms through which FST inhibits KCl-induced vessel contraction in the SHR. Resistance mesenteric arteries taken from SHR or normotensive control WKY rats were tested in response to KCl using wire myography. Primary vascular smooth muscle cell (VSMC) cultures were established from WKY and SHR vessels. The fluorescent calcium sensor dye Fluo-4 AM and potassium tracking dye IPG-1 were then used to examine ion levels in the VSMCs. To determine whether FST effects were activin-mediated, neutralizing antibodies against activin A and B were used. Only activin A neutralization in the SHR reduced KCl-induced contraction as well as intracellular calcium rise, similarly to FST. Activin A (30 minute treatment) augmented KCl-induced contraction in both WKY and SHR vessels, but this was more pronounced in the SHR. There was an augmented KCl induced-intracellular calcium rise in SHR VSMC compared to WKY, which was decreased by FST. Inhibiting release of intracellular calcium stores did not attenuate KCl-induced calcium influx that was augmented by activin A or reduced by FST, but both of these effects were inhibited in calcium-free conditions. FST also significantly lowered the augmented KCl-induced intracellular potassium increase seen in SHR VSMC. Overall, FST reduces augmented KCl-induced contraction and rise in calcium and potassium levels in SHR vessels and VSMC. Taken together, these data suggest that FST may modulate L-type voltage gated Ca^{2+} channel (LTCC) or K-ATP channel activity. Neutralization studies support an important role for activin A, but not activin B, in mediating FST effects. Further studies will examine the mechanism by which FST modulates calcium influx.

ACKNOWLEDGEMENTS

I would like to acknowledge and give my deepest thanks for the unwavering support provided by my supervisors, Dr. Joan Krepinsky and Dr. Jeffrey Dickhout, throughout my entire project. Over the past two years, Dr. Krepinsky has been a pillar of motivation and her continual guidance has been integral to shaping my research skills and personal development. I am forever indebted to her for her mentorship. This project would also not have been possible without the immense expertise provided by Dr. Jeffrey Dickhout. I am beyond grateful for his brilliant comments, suggestions and persistent encouragement as it has catalyzed my personal and professional growth. I could not have asked for better supervisors for my Master's studies.

I would also like to extend my sincere appreciation to my committee member, Dr. Luke Janssen, for his insightful suggestions and vast knowledge on the topic of smooth muscle physiology throughout our meetings. Your support, questions and experimental recommendations truly strengthened this project as well as my research skills, and for that I thank you.

A heartfelt thanks goes to my lab friends, especially Ann and Vincent, who provided me with courage, experimental expertise and great company every day. Thank you for teaching me techniques, sharing your knowledge and answering any inquiries I had. My gratitude extends to the rest of the Krepinsky lab whose help has also been invaluable.

Lastly, my deepest appreciation is towards my family whose love and support kept me going on in this journey. Thank you for cheering me on every step of the way!

TABLE OF CONTENTS

DECLARATION OF ACADEMIC ACHIEVEMENT

The study has been designed by Dr. Krepinsky and Dr. Dickhout and I took the lead in running experiments, analyzing and interpreting data as well as writing the thesis. Vincent Lu has done all the animal sacrifices for the experiments and Ann Kuganathan has contributed her suggestions for experimental set-ups. Renzhong Li has assisted in the conducting of the CAGA12 Luciferase Assay.

1.Introduction

1.1 Essential Hypertension

Hypertension (HTN) remains one of the world's leading causes of death and morbidity worldwide [1]. It affects more than four billion people globally, but only a quarter of adults with HTN have their condition under control with anti-hypertensive medication [2]. By definition, HTN is having persistent readings of a systolic blood pressure of 130 mmHg or more with or without a diastolic blood pressure of greater than 80 mmHg [3]. There are two types of HTN that make up the majority of hypertensive cases; primary or essential HTN and secondary HTN [4]. Primary or essential HTN constitutes 95% of all hypertensive cases and represents idiopathic disease, where consistently high blood pressure results from no identifiable cause [5]. Secondary HTN on the other hand, makes up only about 5% of cases and results from an underlying medical condition such as renal disease, congenital heart disease or endocrinological disorders [6]. Management of secondary HTN often includes medical and/or surgical intervention, lifestyle modifications as well as treatment of the causative renal or endocrine disorder [7]. Treatment of esential HTN is often more complex as its cause could be multifactorial, but it often includes drug therapy such as calcium channel blockers, angiotensin-converting enzyme inhibitors, beta blockers and diuretics [8]. Although traditional anti-hypertensive agents typically work well in managing both forms of HTN, there are patients with resistant HTN whose blood pressure remains high despite the use of maximally tolerated doses of multi-drug treatment plans [9]. Since many hypertensive cases don't meet targets for blood pressure with medication, this highlights the ongoing necessity for the development of new HTN medication.

1.2 Animal Models of Essential Hypertension

Spontaneously hypertensive rats (SHRs) represent one of the most widely used animals for studies of essential HTN [10]. SHRs are the preferred model for HTN studies due to the reliability of their developing HTN as they have a genetic predisposition to the disease [10]. Furthermore, they do not require surgical intervention or external factors to induce HTN and this spontaneous onset of HTN is reflective of essential HTN in humans which lack an identifiable cause [11]. The SHR strain was originally produced by Okamoto and Aoki in the 1960s through genetic inbreeding of Wistar-Kyoto (WKY) normotensive rat models with high blood pressure [12]. HTN begins to develop in these inbred rats at about 6 weeks of age and reaches a stable level of HTN as adults from 12-19 weeks of age [13]. WKY rats serve as an ideal normotensive control to SHRs in studies of essential HTN due to their genetic similarity, reducing genetic variability as a potential confounding variable when assessing physiological parameters [14].

1.3 Hypertension Pathophysiology

Abnormalities in physiological mechanisms responsible for the maintenance of normal blood pressure can give rise to the manifestation of HTN. Most patients with essential HTN can have a normal cardiac output (CO) but increased total peripheral resistance (TPR), giving rise to increased blood pressure (BP) as described by the equation BP= CO x TPR [15]. Small arterioles are typically what determine peripheral resistance, as opposed to smaller capillaries or larger arteries [15]. Resistance vessels such as mesenteric arteries contribute significantly to peripheral resistance and allow for the direct study of vascular function in HTN [16]. Prolonged smooth muscle contraction in HTN can induce structural changes such as thickening of the vessel wall as well as functional changes including an irreversible rise in vascular resistance [15]. Endocrine

systems such as the renin-angiotensin system are also implicated in the pathophysiology of HTN. In the renin-angiotensin system, renin converts angiotensinogen to angiotensin I which is rapidly converted to angiotensin II in the lungs and kidneys by angiotensin-converting enzyme. Angiotensin II can not only directly cause increased blood pressure due to its vasoconstrictive properties but also stimulates the release of aldosterone that causes sodium and water retention and consequently further increased blood pressure [15]. Furthermore, endothelial dysfunction can also contribute to the development of HTN as vascular endothelial cells produce local vasoactive molecules such as nitric oxide and the vasoconstrictor peptide, endothelin-1 [17]. When endothelial function is impaired, reduced nitric oxide production or increased endothelin production can cause reduced vasodilation or increased vasoconstriction, respectively [17]. These changes can alter the structure and function of the underlying smooth muscle cell layer by causing medial hypertrophy and hypercontractility [18, 19]. Additionally, oxidative stress in the form of elevated reactive oxygen species can play an important role in the development of HTN [20]. The primary source of vascular superoxide is nicotinamide adenine dinucleotide phosphate (NADPH) oxidase, specifically when activated by hormones such as angiotensin II and endothelin-1 [20]. Increased ROS production can also contribute to vasoconstriction by raising intracellular calcium levels, thereby further exacerbating HTN manifestation [20]. Overall, it is clear that a multitude of mechanisms contributing to vascular structural and functional changes are at play in the development and maintenance of HTN.

1.4 Smooth Muscle Contraction

Signalling molecules of the Rho/Rho-associated protein kinase (ROCK) pathway and smooth muscle cell ion channels such as LTCCs are heavily involved in the constriction of smooth muscle [21]. The Rho/ROCK pathway can be activated by agonists such as potassium chloride (KCl) as well as hormones such as angiotensin II and endothelin-1 [22,23]. In vascular smooth muscle, KCl has been suggested to enhance activation of the Rho/ROCK pathway by increasing calcium influx into cells [24]. The contribution of depolarization and subsequent calcium influx of KCl to Rho/ROCK pathway activation can be due to enhanced activity of Rho-GTPase activating protein [25]. The Rho/ROCK pathway can also be activated through G-protein coupled receptor signalling when certain hormones, neurotransmitters and ligands bind to their respective G-protein coupled receptor, triggering G-protein activation and causing the Gα subunit to dissociate from the Gβγ subunits and activating Rho GTPases [26, 27]. In their active state, Rho-GTPases such as RhoA-GTP bind to and activate ROCKs [28]. Activated ROCKs phosphorylate downstream substrates such as myosin phosphatase target subunit 1 (MYPT), leading to inhibition of myosin light chain phosphatase, an enzyme that dephosphorylates myosin light chain (MLC) [28]. Phosphorylation of MLC increases the activity of myosin ATPase, allowing for actin-myosin interactions and consequently smooth muscle cell contraction [28].

It is important to note that phosphoinositide signalling can also play an important role in calcium handling and smooth muscle contraction [29]. As shown in diagram 1, once G-protein coupled receptors are activated, some can activate phospholipase C (PLC) enzymes such as PLCβ [30,31]. PLCβ can catalyze the hydrolysis of phosphatidylinositol 4,5-bisphosphate (PIP2), a membrane phospholipid, into secondary messengers: inositol trisphosphate (IP3) and

diacylglycerol (DAG) [30,31]. IP3 as a second messenger can bind to specific IP3 receptors in the endoplasmic reticulum (ER), a site of calcium storage [30,31]. This binding can trigger the release of calcium ions from the ER into the cytoplasm [30,31]. Calcium ions in the cytoplasm can then bind to and activate calmodulin which can then activate myosin light chain kinase [30,31]. This leads to the phosphorylation of the myosin regulatory light chain, triggering the formation of cross-bridges with actin filaments and allowing for acto-myosin interactions and contraction [30,31].

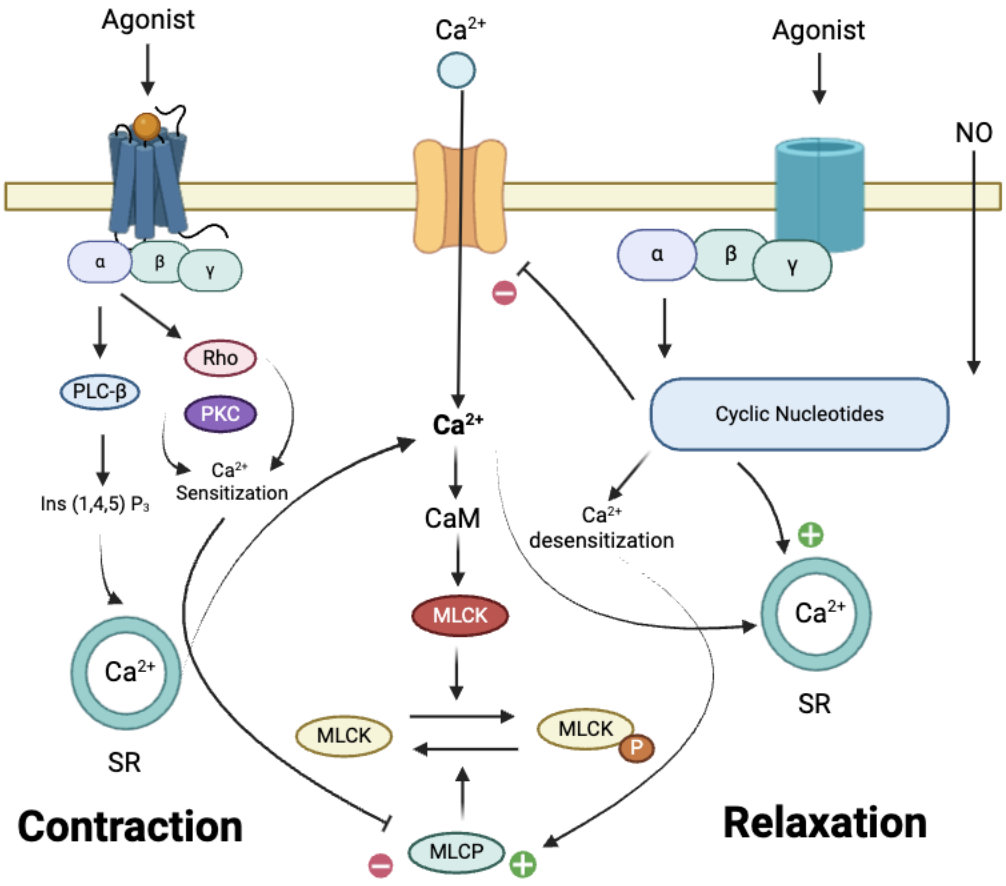

Diagram 1. General mechanisms of smooth muscle contraction and relaxation. Figure made using Biorender and modified from Puetz et al. (2009).

Ion channels including potassium and calcium channels contribute significantly to vascular smooth muscle contraction and therefore, blood pressure regulation. A study by Moosmang et al.

in 2003 showed that smooth muscle-specific inactivation of the Cav1.2 LTCC subunit gene in mice (SMAKO) reduced isometric force generation in aortic rings and lowered mean arterial pressure from 120 ± 4.5 to 87 ± 8 mmHg compared to control [33]. Depolarization of the smooth muscle cells through agonists such as KCl is sensed by LTCCs, causing them to open, allowing calcium influx down its concentration gradient and leading to activation of the contractile apparatus described above [34]. Potassium channels such as voltage-gated potassium channels (Kv) and ATP-sensitive potassium channels (K-ATP) are also involved in smooth muscle contraction and regulation [35]. Voltage-gated potassium channels are typically active at the resting membrane potential of vascular smooth muscle, allowing potassium to efflux. Closure of these channels can cause membrane depolarization and subsequent vessel constriction [35]. K-ATP channels, on the other hand, are sensitive to intracellular ATP levels and when there is an increased amount of ATP, they tend to remain closed [36]. However, in situations of energy depletion, K-ATP channels are opened, causing potassium efflux, membrane hyperpolarization and subsequent smooth muscle relaxation [36]. Diagram 2 visually showcases this phenomenon in a smooth muscle cell [37].

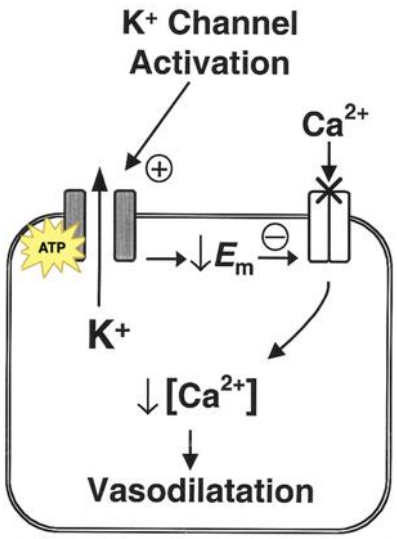

Diagram 2. Overview of the role of ion channels in smooth muscle cell relaxation. Figure modified from Sobey (2001).

1.5 Activins and Follistatin and their role in HTN

The study of activins are of particular interest for their potential role in HTN. Activins are members of the TGF-β family of cytokines and were initially isolated from gonads and in addition to acting as modulators of follicle-stimulating hormone secretion exert control over physiological processes such as cell proliferation, differentiation, metabolism and immune responses [38, 39]. Activin A and B signaling is initiated when activin binds to specific cell surface receptors consisting of type I and type II serine/threonine kinase receptors [40]. Subsequently, the type II receptor phosphorylates and activates the type I receptor which phosphorylates Smad 2 and 3 proteins which form complexes and translocate into the nucleus [40] Inside the nucleus, the Smad complex serves as a transcription factor and modules expression of target genes involved in the aforementioned biological processes [40].

FST is a secreted protein that can effectively neutralize several activins [40]. Two FST molecules can bind to an activin dimer with high affinity and sterically hinder the interaction between the activins and their receptors [41]. FST causes activin internalization but it can also contribute to activin degradation by interacting with its associated cell-surface receptors [41]. By doing this, FST essentially inhibits the biological function of activins [40]. There are three isoforms of FST including FST 288, FST 303 and FST 315 which all differ in length at the C-terminus [42]. The cell-surface binding ability of each isoform is significantly different, with the FST 288 isoform binding with the highest affinity followed by FST 303 and finally, FST 315, the

circulatory form of FST [43]. Inhibition of activin biological function is closely correlated with surface binding activity, making the FST 288 isoform the most potent inhibitor of activins [43].

Activins have been shown to be implicated in the pathogenesis of HTN. Of most relevance is the findings of a longitudinal study by Tsai et al., in which serum activin A levels were shown to be significantly higher in patients with essential HTN compared to normotensive controls [44]. Another study measured serum activin A in pregnant women and found activin A to be elevated in pregnant women with pregnancy-induced HTN and those with pre-eclampsia, which is pregnancy-onset HTN with increased levels of protein in urine, compared to healthy pregnant women [45].

1.6 Relationship Between Activins and Ion Channels

Activin A has also been found to induce functional changes in ion channels that are critical to smooth muscle contraction and thus may contribute to HTN pathophysiology, such as the K-ATP and LTCCs [46]. A study done by Mogami et al. on HIT-T15 insulinoma cells used patch-clamping to determine whether activin A modified potassium currents through the K-ATP channel [46]. They found that activin A inhibited K-ATP channel currents as K-ATP channel activity was significantly reduced after the addition of activin A into the bath solution and this effect was seen in approximately 10 minutes [46]. Activin A also induced depolarization in the cells that was followed by a burst of action potentials and increased calcium levels in the cytoplasm which was observed within 5 minutes of activin A application to the cells [46]. Lastly, they reported the role of activin A in modulating calcium entry through the LTCC as activin A enhanced inward barium current, an effect that was blocked with nifedipine [46]. However, the exact mechanism through which activin A regulates the activity of the LTCC is mostly unknown.

2. Objectives of Study

2.1.0 Rationale

The lab has previously shown that chronic FST (288 isoform) treatment (0.075 mg/kg) lowered blood pressure and improved vascular remodelling of mesenteric arteries in SHRs [47]. We have also identified that short-term (30 minutes) FST treatment lowered potassium-induced contraction in both WKY and SHR in ex-vivo wire myography studies. Activin A has been shown to inhibit K-ATP currents and induce calcium entry via LTCCs in insulinoma cells [46]. Other studies have also determined that activin A enhanced the activity of LTCCs in neuroblastoma C1300 cells [48]. In vascular smooth muscle, K-ATP channels play a major role in the hyperpolarization of smooth muscle cells [49]. Additionally, K-ATP channel subunits, Kir 6.2 and SUR2 have significantly greater expression in SHRs compared to normotensive WKY [50]. LTCCs also act as the main pathway through which excitation-contraction coupling occurs in small resistance vessels such as the ones in the rat mesenteric bed [51].

2.1.1 Hypothesis

I hypothesize that FST lowers potassium-induced contraction through the blockage of intracellular calcium entry through LTCCs.

2.1.2 Aims

The specific aims are:

1.) Test whether FST inhibits calcium influx into vascular smooth muscle cells and whether this calcium influx is activin-mediated.

2.) Examine whether FST modulates intracellular potassium levels in vascular smooth muscle cells and whether these intracellular potassium levels are activin-mediated.

3.) Investigate whether FST effects on lowering contraction are generalizable to agonists other than KCl such as phenylephrine and serotonin.

3. Methods

3.1 Cell explant and cell culture

All studies were approved and conducted in accordance with the McMaster University ethical guidelines on animal care. Primary vascular smooth muscle cell cultures were established from the superior mesenteric artery of WKY and SHR using the cell explant technique. In the tissue preparation process, superior mesenteric arteries were dissected by removing adjacent fat and connective tissue under a dissecting microscope. The isolated arteries were then cut along their length and placed in a smaller petri dish filled with phosphate-buffered saline (PBS), leaving some adipose tissue for ease of handling. A 1:20 dilution of 100X antibiotic-antimycotic (Gibco) was prepared for immersing the arteries in the antibiotic-antimycotic solution. After rubbing along the endothelium with a cotton swab to remove the endothelium, the arteries were segmented into six pieces and placed in a 6-well plate with a UV-sterilized glass cover slip on top of each artery as well as one drop of 100% fetal bovine serum (FBS) in each well. The space around the cover slips was filled with 2 mL of warmed low glucose DMEM media containing 100µg/mL streptomycin, and 100µg/mL penicillin and 10% FBS. Each plate was stored at 37℃ in a 95% O2, 5% CO incubator for 7-10 days. Once cell growth was observed and reached 80% confluence, they were passaged into 10 cm dishes at $3x10^5$ cells per plate. Cells have been passaged on a weekly basis once they have reached 80% confluency and plated for experiments,

as necessary. Cells from passages 5-15 have been used for more recent assays and a frozen inventory of cells from early passages has been replenished for ongoing and future experiments.

3.2 Fluorescent Calcium Assays

Cells were plated at a density of 20,000 cells per well in a 96-well plate with a clear bottom (clear bottom Optilux, BioLynx) the day before the experiment to ensure that the cells would reach approximately 100% confluence by the day of the assay. On the day of the assay, a 50 µg vial of the Fluo-4 calcium indicator (Catalog # F14201, Lot # 32847W, Thermo Fischer) was diluted in 91.16 µL DMSO to obtain a concentration of 0.5 mM. A 5 µM concentration of Fluo-4 was then prepared by mixing 10 µl of the previously made 0.5 mM Fluo-4 and 10 µl of 20% pluronic acid (Catalog #: 7601A, ION Biosciences), then diluting in 1 mL HEPES buffered Hank's Balanced Salt Solution (HHBSS). Cells were washed with HHBSS prior to loading with 5µM Fluo4-AM for 45 minutes at room temperature. The plate was covered with aluminum foil as the dye is light-sensitive. To prevent dye compartmentalization, staggered loading and incubation of the dye were performed for each treatment group in a single experiment. Following the dye-loading step, cells were washed three times with HHBSS. Subsequently, cells were incubated at 37°C for 15 minutes for esterase activation of Fluo4-AM, and a heating plate on the microscope was pre-warmed during this step. Additionally, Follistatin 288 (FST) at a concentration of 500 ng/ml was introduced during this incubation period. Afterward, the plate was transferred to the microscope for fluorescence imaging, beginning typically with a 40-second baseline reading at excitation of 488 nm (FITC) with a frame rate of 1 frame per second. KCl at a concentration of 125 mM was then added to a well, and fluorescence readings were taken second for approximately 3-6 minutes. In certain dose-response experiments, varying concentrations of KCl were also used. Stimulation

of the cells with dH_2O acted as vehicle since our KCl stock had been made in dH_2O. Subsequent treatment groups followed a similar procedure, starting with a baseline reading and then continuous readings after the addition of the respective solutions. If required, positive and negative controls were included as ionomycin (10µM) and calcium-free HHBSS, respectively. Finally, data analysis was performed using the Metamorph software.

3.3 Fluorescent Potassium Assays

Cells were plated at a density of 20,000 cells per well in a 96-well plate with a clear bottom (clear bottom Optilux, BioLynx) the day before the experiment to ensure that the cells would reach approximately 100% confluence by the day of the assay. On the day of the assay, a 50 µg tube of the IPG-1 potassium indicator (Catalog # 3041F, ION Biosciences) was dissolved in 25 µl DMSO to obtain a concentration of approximately 2 mM. Then, a final concentration of 5 mM IPG-1 was obtained by mixing 2.5 µl of the previously made 2 mM IPG-1 and 10 µl of of 20% pluronic acid (Catalog #: 7601A, ION Biosciences), then diluting in 1 mL HHBSS. IPG-1 is a fluorescent potassium tracker that detects small changes in intracellular potassium and has an excitation/emission of 525 nm/545 nm. Subsequently, cells were washed with HHBSS prior to loading with IPG-1 AM for 60 minutes at 37 °C. For FST treatment, an additional incubation at 37 °C for 30 minutes prior to imaging was completed. The plate was also covered in aluminum foil due to the light-sensitive nature of the dye. Cells were then transferred to the microscope for fluorescence imaging, beginning with a 40-second baseline reading at 488 nm (FITC) with a frame rate of 1 frame per second. KCl at a concentration of 125 mM was then added to a designated well column, and fluorescence readings were taken every second for approximately 3-6 minutes. The acquired data were subsequently analyzed using Metamorph software.

3.4 Membrane Potential Sensing Dye

Cells were plated at a density of 20,000 cells per well in a 96-well plate with a black/clear bottom (clear bottom Optilux, BioLynx) the day before the experiment to ensure that the cells would reach approximately 100% confluence by the day of the assay. On the day of the assay, a 100 nM $DiBAC_4(3)$ dye-loading solution was made in HHBSS (Catalog #: B438, Thermo Fischer) with 0.05% Pluronic F-127 (Catalog #: 7601A, ION Biosciences). $DiBAC_4(3)$ is a cell permeant, voltage-sensitive dye that is anionic at its resting state. As cells depolarize, the $DiBAC_4(3)$ dye tends to accumulate intracellularly, leading to increased fluorescent signal. Cells were loaded with the $DiBAC_4(3)$ dye for 30 minutes at 37 °C. Select wells were also treated with 500 ng/ml of FST during this step. The plate was covered in aluminum foil due to the light-sensitive nature of the dye. Immediately after the incubation period, cells were transferred to the microscope for fluorescence imaging, beginning with a 40-second baseline reading at 488 nm (FITC) with a frame rate of 1 frame per second. KCl at a concentration of 125 mM was then added to a designated well column, and fluorescence readings were taken every second for approximately 3-6 minutes . The acquired data were subsequently analyzed using Metamorph software.

3.5 CAGA12 Luciferase

Kidney mesangial cells were plated on a 6-well plate at a seeding density of 50,000 cells/well the day before the start of the experiment. The following day, cells were transfected with CAGA12 luciferase constructs and β-gal. Following a 18-24 hour period, the cells were then placed in starvation medium for 24 hours. The next day, cells were treated for 24 hours with either 0.5 ng of

TGF-β , 1 μg/ml of TGF-β neutralizing antibody (R&D Systems) or 1 μg /ml of mouse IgG (Leinco Technologies). During harvesting, cells were lysed with reporter lysis buffer (Promega) and placed in -80 °C overnight. Cell lysates were then scraped and centrifuged before measuring luciferase activity with the Luciferase Assay System (Promega) using a SpectraMax Microplate Reader (Molecular Devices) which measures luminescence. The β-Galactosidase Enzyme Assay System (Promega) was used to normalize sample values and this was done at 420 nm using a plate reader (SpectraMax Plus 384, Molecular Devices).

3.6 Immunohistochemistry

Vessels from the mesenteric bed were harvested, and fixed in 4% paraformaldehyde solution (Biolynx), for 24 hours prior to processing and embedding. Paraffin-embedded WKY and SHR vessels were sectioned at 4μm, deparaffinized and stained using a phospho-SMAD3 antibody that detects phosphorylation site Thr853 (1:1500, Novus) or p-MYPT antibody (1:200, Cell Signalling). Antigen retrieval was done with citric acid steaming for 15 minutes for p-SMAD3 or in proteinase K (40 μg/ml) for 10 minutes, prior to blocking for 60 minutes (1:20) and overnight primary antibody incubation. Images were captured using the Olympus BX41 microscope at 40x and then quantified using ImageJ software.

3.7 Wire Myography

Mesenteric tissue was obtained from rats in accordance to the McMaster University animal care guidelines. Initially, the fat tissue surrounding vessels was dissected to better expose the first-order mesenteric vessels. Arterial rings were cut at an approximate length of 2 mm and were submerged in HBSS. Vessels treated with FST (500 ng/ml), neutralizing activin A and B

antibodies (3.5 µg/ml, Catalog #: MAB3381 and MAB659-sp, R&D Systems), Mouse IgG (3.5 µg/ml, Leinco Technologies), TGF-β1 neutralizing antibody (R&D Systems), and SB 431542, an activin receptor inhibitor (5 µM, Tocris), were transferred to a 96-well plate containing 100 µl of low glucose DMEM media and incubated for 30 minutes at 37 °C. Following treatment, vessels were threaded with two stainless tungsten steel wires at 4 cm lengths (Goodfellow). The vessels were subsequently positioned in myograph chambers (Radnotic LLC, USA), each filled with 5 mL of HBSS while ensuring the proper oxygen supply and temperature (37 °C). The vessels with threaded wires were then mounted onto the myograph organ chambers and set to 0.5 g baseline tension. Following a 30-minute period at 0.5 g, vessels were challenged with varying doses of agonists such as KCl, Angiotensin II, BayK 8644 (Tocris) and FPL 64176 (Tocris) to observe vessel reactivity. Contractility measurements were quantified as the force generated by vessel contractions in the units of grams tension, using the WinDaq Lite 0 software.

Drug	**Catalog # and Source**	**Function**
Anti-activin A antibody	Catalog #: MAB3381, R&D Systems	Neutralizes activin A effects
Anti-activin B antibody	Catalog #: MAB659-sp, R&D Systems	Neutralizes activin B effects
Mouse IgG	Catalog #: I-117, Leinco Technologies	IgG control for antibody treatment experiments
TGF-β1 neutralizing antibody	Catalog #: MAB1835, R&D Systems	Neutralizes TGF-β1 effects
SB 431542	Catalog #:1614, Tocris	Activin and TGF-β-receptor inhibitor (selectively inhibits of Alk4/5/7)

BayK 8644	Catalog #:1546, Tocris	Agonist of LTCC; alters voltage dependence of channel activation to more negative potentials.
FPL 64176	Catalog #: 1403, Tocris	Potent agonist of LTCC; changes channel selectivity, alters blocker efficacy and enhances calcium tail currents.

Table 1. Outlined information on the drugs used for experimentation, their sources and exerted functions.

3.7 Statistical Analysis

A one-way or two-way ANOVA was used to assess significant differences between two or more groups. A one-way ANOVA was used for contractility experiments where there was one independent variable such as treatment while a two-way ANOVA was used for cell assays with two independent variables such as treatment and time. Tukey and Sidak's post hoc analyses were used to compare differences between pairs of group means. ImageJ was used for the quantification of immunohistochemistry experiments and Metamorph was used for analysis of calcium, potassium and membrane potential sensing assays. GraphPad Prism was used for the analysis of all data. Statistical significance was set to $p<0.05$ and data are represented as mean ± SEM.

4. Results

4.1 Effects of activin A and activin B neutralization in WKY and SHR vessels

In order to examine the effect of activin neutralization on potassium-induced contraction, first-branch mesenteric vessels were dissected from 30-week-old WKY and SHRs and treated for 30 minutes with activin A or B neutralizing antibodies (3.5 µg/ml) or IgG1 control (3.5 µg/ml). As shown in Figure 1A, neutralization of activin A and Activin B did not produce a statistically significant change in the KCl-induced contraction in WKY vessels. In Figure 1B, SHR vessels treated with the activin A neutralizing antibody showed statistically significant reductions in potassium-induced contraction that were similar to the contractility measurements obtained from FST pre-treated vessels shown in other contractility set-ups, while activin B neutralization had no effect on lowering contraction. This suggests that in the SHR, FST may be mediating its effects through activin A neutralization, as opposed to direct effects on Activin B. In WKY vessels, both activin A and Activin B seem to contribute similarly to potassium-induced contraction. Although the neutralization of both activins reduced contraction compared to IgG-treated vessels, this effect was not statistically significant.

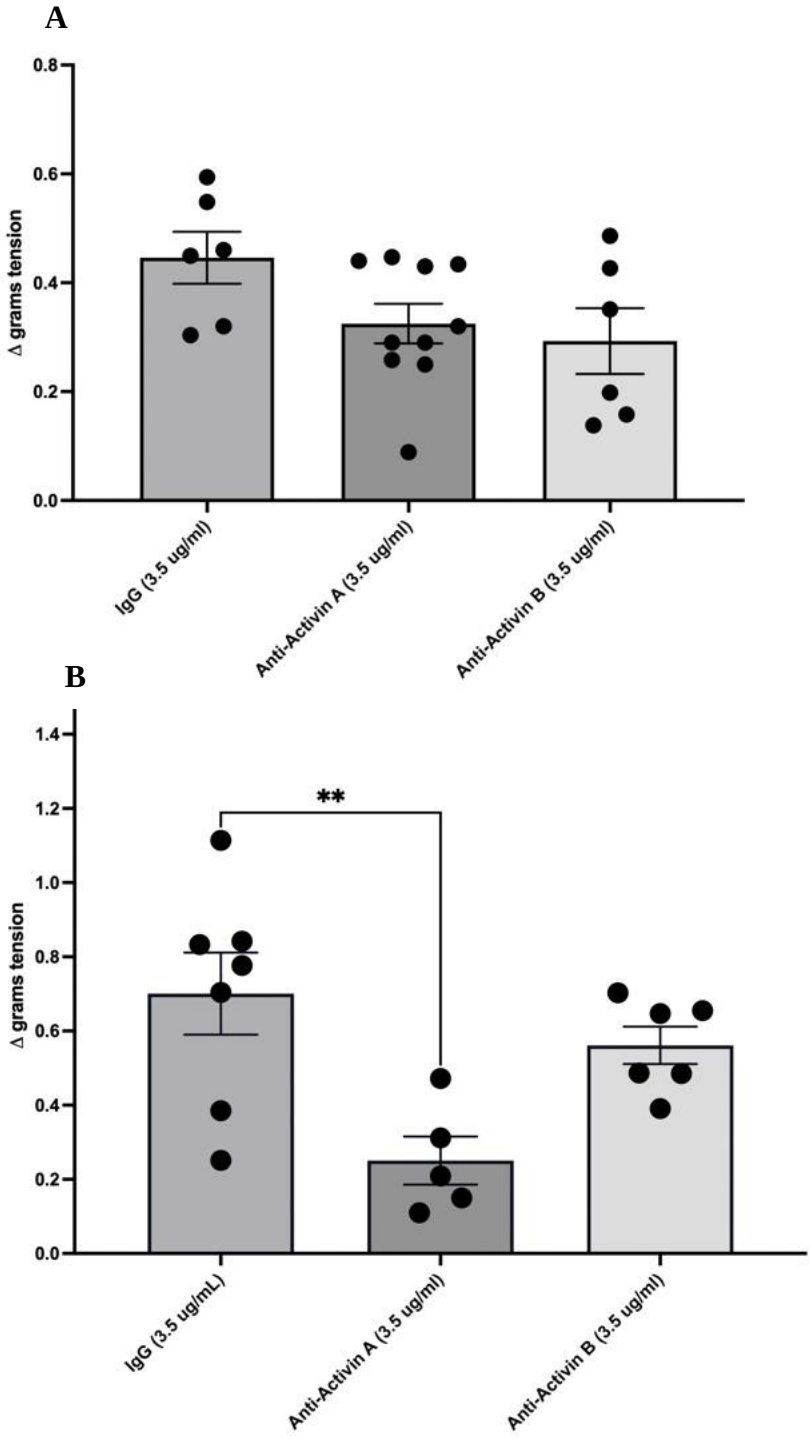
A
0.8
0.6
0.4
0.2
0.0
Δ grams tension
IgG (3.5 ug/ml)
Anti-Activin A (3.5 ug/ml)
Anti-Activin B (3.5 ug/ml)
B
1.4
1.2
1.0
0.8
0.6
0.4
0.2
0.0
Δ grams tension
**
IgG (3.5 ug/mL)
Anti-Activin A (3.5 ug/ml)
Anti-Activin B (3.5 ug/ml)

Figure 1. Contractility measurements in gram tension values from 30-week-old WKY (A) vessels acutely incubated (30 minutes) with mouse IgG1 (3.5 µg/mL), FST (500 ng/ml) or neutralizing activin A or Activin B antibodies (3.5 µg/mL), then challenged with KCl (125 mM) show significant reduction in contraction only with FST treatment compared to control. (B) Activin A neutralization and FST treatment similarly reduced KCl-induced contraction in SHR vessels compared to Activin B neutralization and IgG control. Analyzed with one-way ANOVA. ** refers to p values of ≤ 0.006.

4.2 Effects of activin A on KCl-induced contraction *in WKY and SHR vessels*

To examine whether treatment with activin A could increase potassium-induced contraction, a dose-dependence of KCl-induced contractions was examined on 30-week-old WKY mesenteric vessels. Since the maximum contraction achieved in this set-up was an increase of 0.8 g, the EC50 of 0.4 g was estimated to be achieved with the 40 mM KCl dose, as shown in Figure 2A. Subsequently, WKY and SHR vessels were treated with 50 ng/ml of activin A and then challenged with 40 mM KCl. As shown in Figure 1B and 1C, activin-A treated vessels show a significant increase in contraction, but this is more pronounced in SHR vessels. Specifically, there was a 1.22-fold increase in contraction with activin A treatment in WKY vessels while there was a 2.15-fold increase in contraction in SHR vessels pre-treated with activin A.

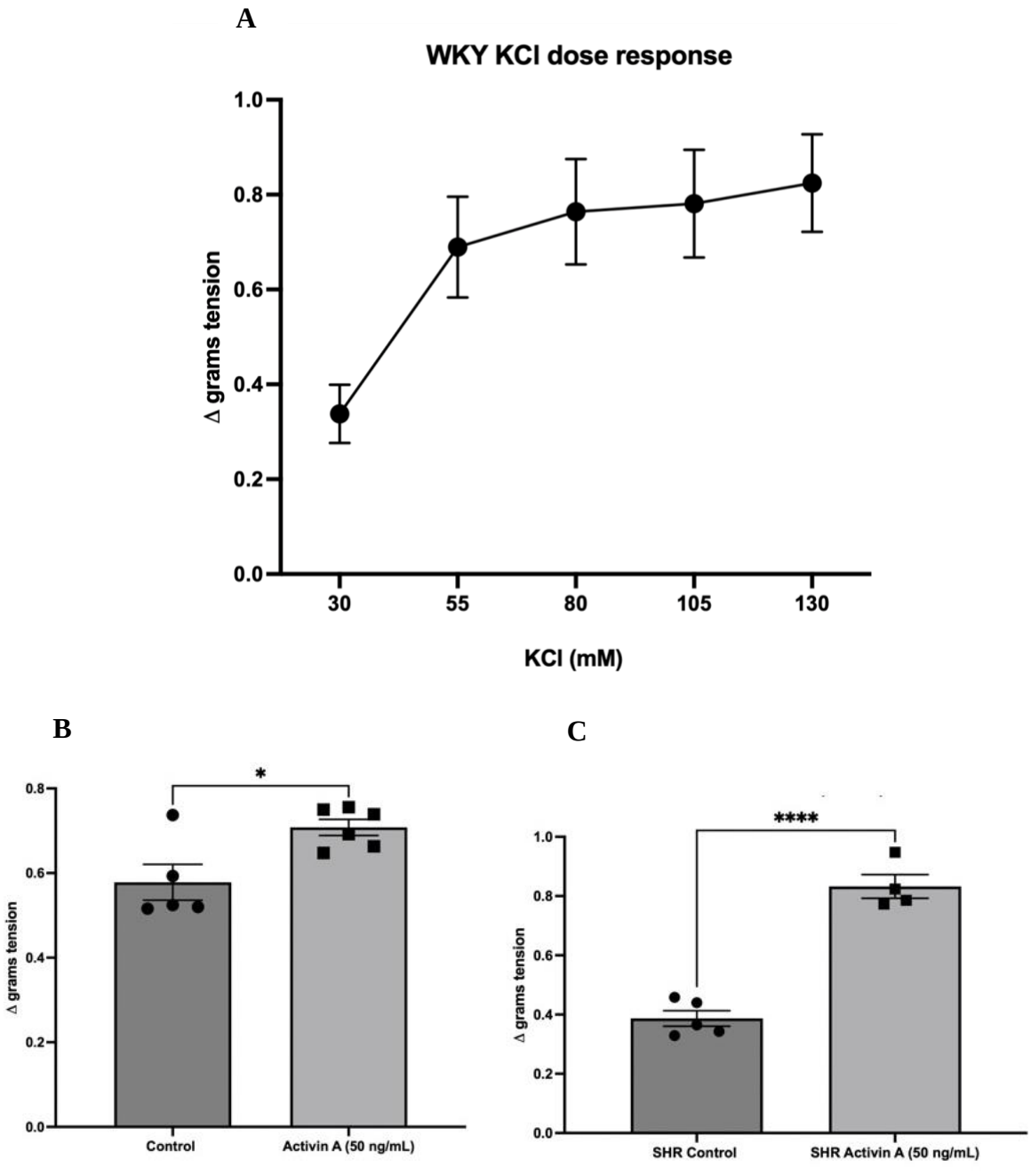
A
WKY KCl dose response
Δ grams tension
1.0
0.8
0.6
0.4
0.2
0.0
30
55
80
105
130
KCl (mM)
B
*
Δ grams tension
0.8
0.6
0.4
0.2
0.0
Control
Activin A (50 ng/mL)
C
****
Δ grams tension
1.0
0.8
0.6
0.4
0.2
0.0
SHR Control
SHR Activin A (50 ng/mL)

Figure 2. Contractility measurements in gram tension values from 30-week-old WKY (A) vessels acutely incubated (30 minutes) with activin A (50 ng/mL) then challenged with KCl in a dose-response manner show step-wise increases in KCl-induced contraction. (B) Activin A treatment significantly increased KCl -induced (40 mM) contraction in WKY vessels compared to control. (C) Activin A treatment also significantly increased KCl -induced (40 mM) contraction in SHR vessels compared to control. Analyzed with one-way ANOVA. *, **** refers to p values of <0.02 and <0.0001, respectively.

4.3 Effects of activin receptor inhibition on potassium-induced contraction in WKY and SHR vessels

Next, we wanted to explore the effect of activin and TGF-β receptor inhibition on potassium-induced contraction in WKY and SHR. Vessels were treated for 30 minutes with either control media, FST (500 ng/mL), SB 431542 (5 μM), an inhibitor of ALK 4/5/7 or FST and SB 431542 simultaneously. Activin A signals through ALK 4, while Activin B and TGF-β signal through ALK 7 and ALK 5, respectively. In Figures 3A and 3B, it is shown that both WKY and SHR vessels treated with FST and SB, respectively, had significantly decreased responses to the KCl challenge (125 mM) to a similar degree. The vessels with concurrent FST and SB treatment were not significantly different than FST and SB treatment, alone. Since SB not only inhibits activin A and B signalling but also TGF-β, a TGF-β neutralizing antibody was used to examine whether the reduced potassium- contraction effects seen with SB 431542 involved TGF-β signalling. In Figure 3C, SHR vessels were treated acutely (30 minutes) with 1 μg/mL of the TGF-β neutralizing antibody, FST (500 ng/ml) or both. Although FST reduced contraction caused

by KCl (125 mM) compared to control, the anti-TGF-β treated SHR vessels showed no decreased response and were not significantly different than control vessels. This implies that the previously seen effects with FST and SB 431542 were through activin signalling inhibition but not TGF-β signalling. Lastly, in order to test the effective neutralization of TGF-β1 with the TGF-β-neutralizing antibody used in previous experiments, a CAGA12 luciferase was conducted and luminescent signal was significantly decreased with the TGF-β-neutralizing antibody when compared to cells treated with TGF-β1 alone (Figure 3D).

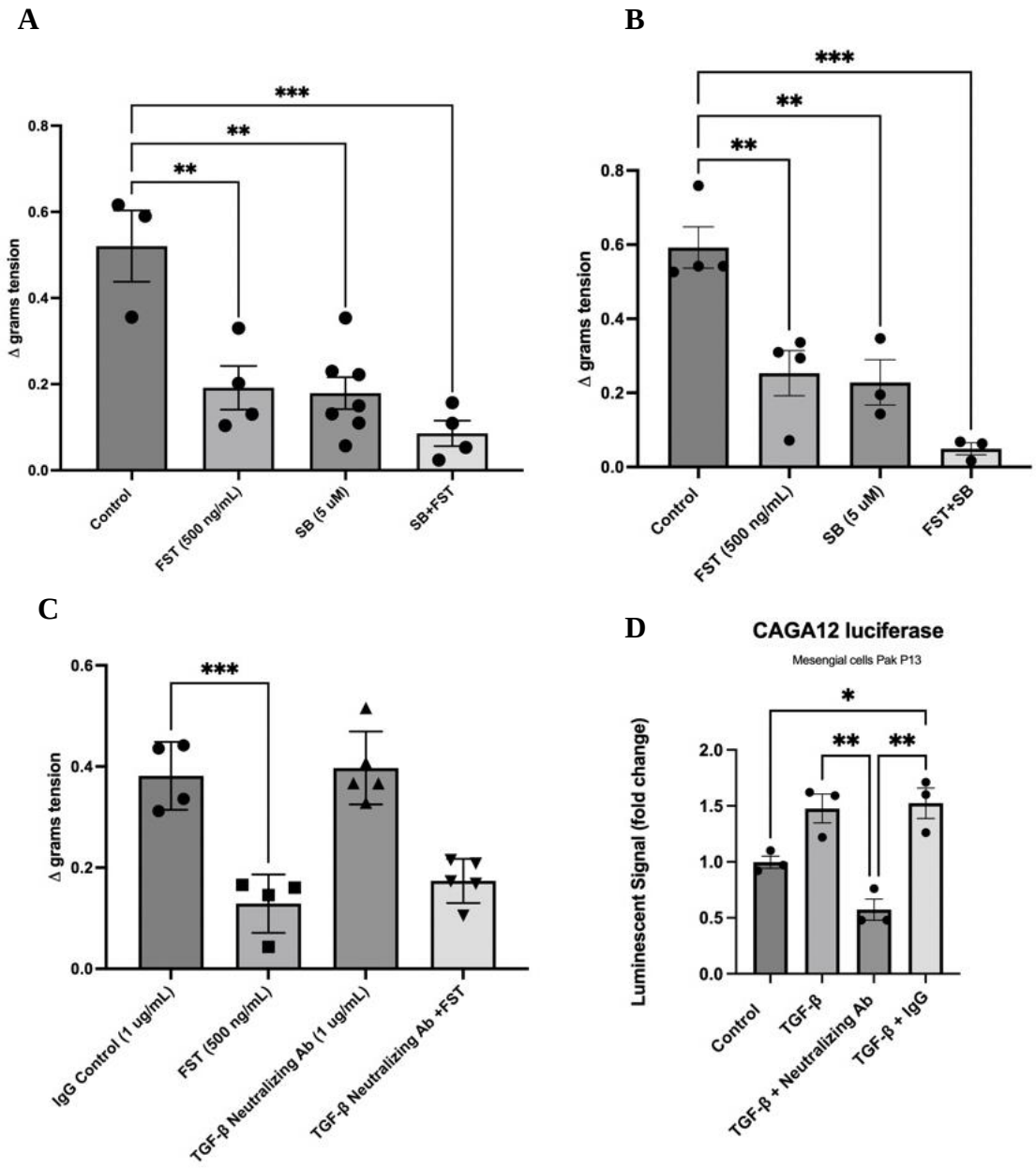

Figure 3. Contractility measurements in gram tension values from 30-week-old WKY (A) and SHR (B) vessels acutely incubated (30 minutes) with FST (500 ng/mL) and/or SB 431542 (5 µM) to inhibit activin and TGF-β1 receptors show similar reductions in KCl -induced contraction (C) SHR vessels treated (30 minutes) with a TGF-β neutralizing Ab (1 µg/mL) show no significant reduction in KCl-induced contraction. (D) Mesangial cells treated for 24 hr with TGF-β1 (0.5 ng)

and TGF-β neutralizing antibody (1 μg/mL) show effective neutralization of TGF-β1 with the antibody as measured through CAGA12 Luciferase. Analyzed with one-way ANOVA. *, **,*** refers to p values <0.04, <0.0045, and <0.003, respectively.

4.4 Effects of LTCC agonist on SHR vessel contraction

In order to determine whether FST reduces potassium-induced contraction by acting directly on the LTCC, an agonist of the Cav1.2 subunit, BayK 8644 was used in our contractility experiments. As shown in Figure 4A, we examined the dose-dependence of BayK-induced contraction (10^{-8} to 10^{-6} M) to determine the optimal dose for inducing contraction. Although the gram tension values vary between the three doses, the 10^{-6} M dose was used in the subsequent set-up. As shown in Figure 4B, SHR vessels were contracted with KCl (125 mM) to assess viability by checking to see if they contract and then washed three times until baseline tension values were reached. The same vessels were then challenged with 10^{-6} M BayK 8644 but the contractile responses were largely variable. In Figure 4C, a time course of SHR vessels challenged with 10^{-6} M BayK 8644 shows peak contraction at 4 minutes and an eventual decrease in response over time. Similarly in Figure 4D, a comparison between the 4-minute and 20-minute mark of SHR vessels contracted with 10^{-6} M BayK 8644 show a decrease in contraction between the timepoints. Due to the extreme variability of responses induced by BayK 8644, FST was not used since we could not be sure whether the lowering of contraction observed with BayK 8644 would be due to FST effects or BayK itself. In Figure 4E, endothelium-denuded vessels were contracted with 125 mM KCl, washed then challenged with 10^{-6} M BayK 8644, to which they had no contractile response. On the same day, vessels with their endothelium intact were stimulated with 125 mM

KCl, washed then challenged with BayK 8644 to which they contracted slightly (Figure 4F). Due to the large range in the contractile responses obtained with BayK 8644 in this experiment compared to previous experiments, FST studies were no longer carried out with BayK 8644. In Figure 4G, SHR control or FST pre-treated vessels were primed with 30 mM KCl for one minute in the myograph organ chamber prior to challenging with 10^{-6} M BayK 8644. Control vessels that showed contraction with 30 mM KCl were not augmented by BayK 8644. Pre-treated FST vessels had significantly decreased KCl-induced contraction and virtually no response to the 10^{-6} M BayK 8644 dose. We are planning to repeat the same experiments completed in Figure G with pressure myography as opposed to wire myography as this may reduce some of the variability seen with BayK 8644.

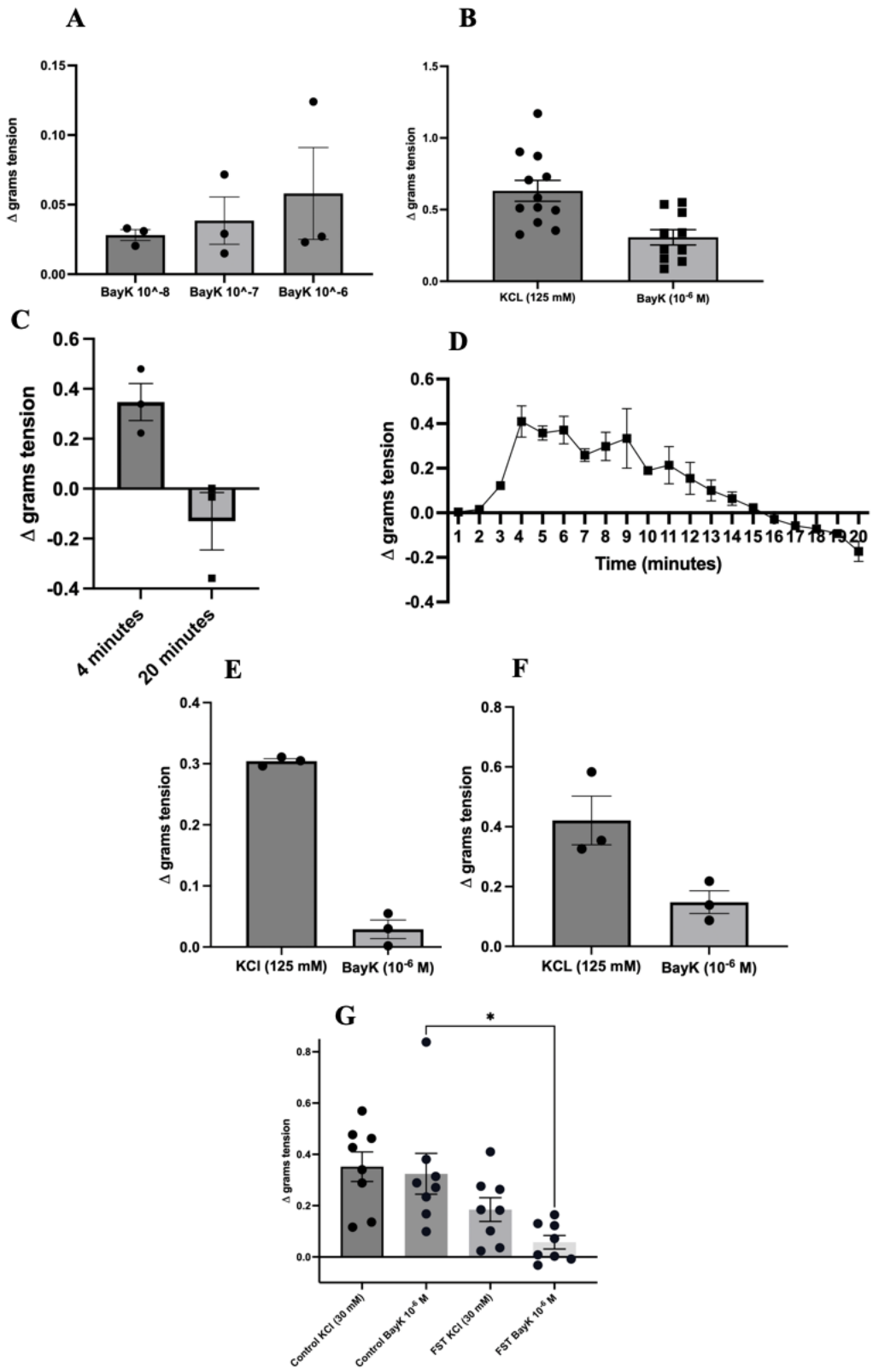
A
Δ grams tension
BayK 10^-8
BayK 10^-7
BayK 10^-6
B
Δ grams tension
KCL (125 mM)
BayK (10-6 M)
C
Δ grams tension
4 minutes
20 minutes
D
Δ grams tension
Time (minutes)
E
Δ grams tension
KCl (125 mM)
BayK (10-6 M)
F
Δ grams tension
KCL (125 mM)
BayK (10-6 M)
G
*
Δ grams tension
Control KCl (30 mM)
Control BayK 10-6 M
FST KCl (30 mM)
FST BayK 10-6 M

Figure 4. Contractility measurements shown in gram tension values from 30-week-old SHR (A) vessels challenged with varying doses of the LTCC agonist, BayK 8644, show increases in contraction with the greatest contraction in the 10^{-6} M BayK 8644. (B) Vessels challenged with KCl (125 mM) then washed 3x and challenged with BayK 8644 (1μM) show varying contractility measurements. (C) Vessels challenged with BayK 8644 (1μM) show a time-dependent increase in contractility, peaking at 4 minutes and steadily decreasing until minute 20. (D) Vessels challenged with BayK 8644 (1μM) show increased contraction at 4 minutes and relaxation beyond baseline at 20 minutes. (E, F) Endothelium-denuded vessels contracted with 125 mM KCl, washed then challenged with 1μM BayK 8644 showed no contraction while endothelium-intact vessels had a slightly higher contractile response. (G)Vessels primed with 30 mM KCl had no augmented contractile response to BayK 8644, FST vessels had reduced response to BayK 8644. Analyzed with one-way ANOVA. * refers to a p value of <0.02.

4.5 Effects of FST on the LTCCs in WKY and SHR vessels

In Figures 5A and 5B, the effects of FST on the LTCC were tested using a different and more potent agonist of the channel, FPL 64176 . Both WKY and SHR vessels treated with FST (500 ng/mL) showed a reduction in KCl-induced contraction (125 mM), but the contraction caused by 10^{-5} M FPL 64176 could not be lowered with 30-minute FST pre-treatment. To determine the specificity of FPL 64176 for the LTCC, SHR vessels contracted with 10^{-5} M FPL 64176 were next relaxed with a known blocker of the LTCC, nifedipine (1 μM). As shown in Figure 5C, vessels relaxed with nifedipine (1 μM) and subsequently challenged with 10^{-5} M FPL

64176 showed no increase in contraction, which supports the specificity of the agonist for the LTCC. FPL 64176 stimulates the LTCC and increases inward calcium current by slowing channel activation and inactivation through changes induced in channel selectivity and blocker efficacy [77]. Overall, these results suggest that FST may not be able to restore the pore alterations of the LTCC caused by FPL 64176.

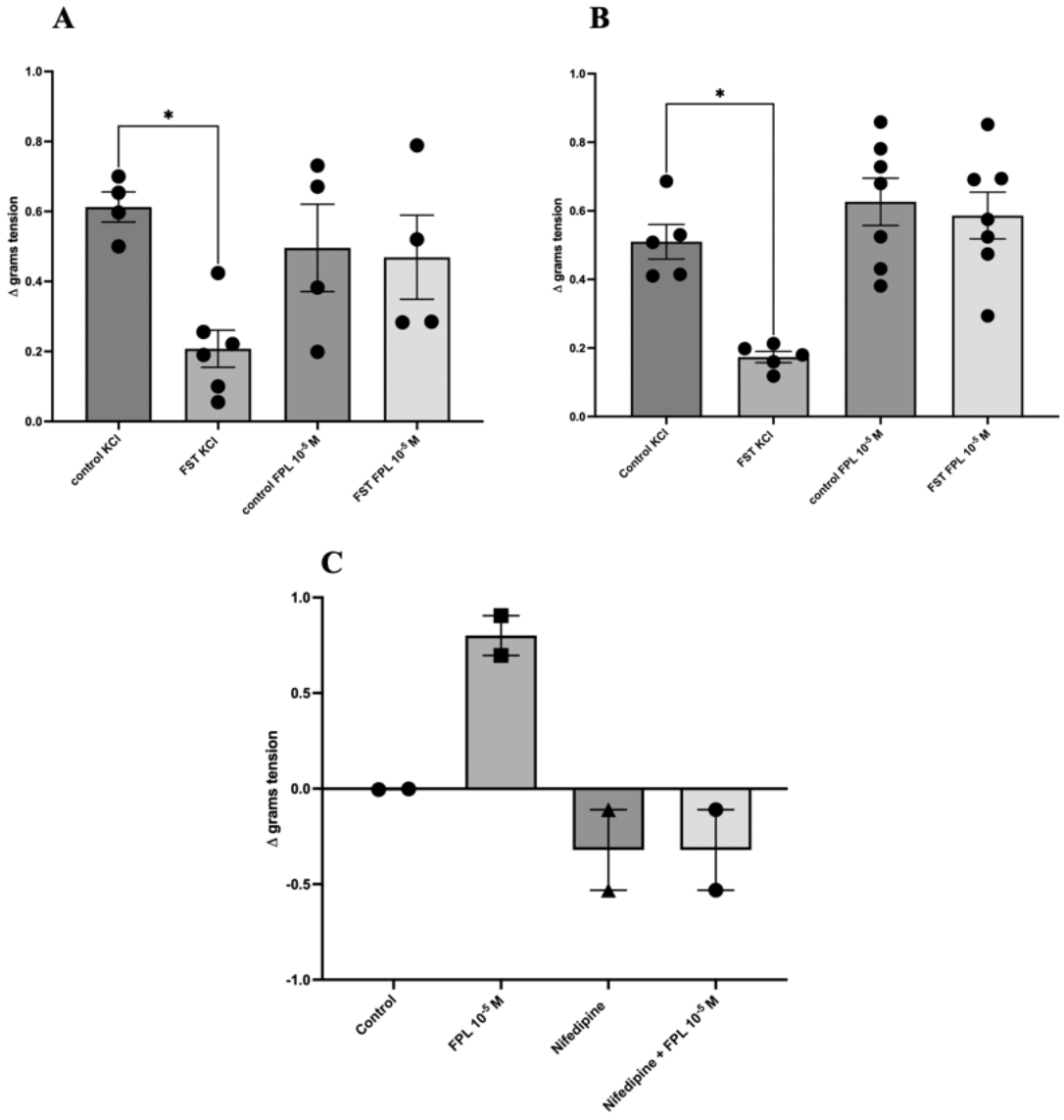

Figure 5. Contractility measurements shown in gram tension values from 30-week-old WKY (A) and SHR (B) vessels acutely incubated (30 minutes) with FST (500 ng/mL), then challenged with KCl (125 mM) show reductions in contraction while vessels challenged with the LTCC agonist-FPL 64176 (10^{-5} M) show similar contractility between control and FST-treated vessels. (C) WKY vessels also directly challenged with FPL 64176 (10^{-5} M) showed a strong contraction that

was blocked by the LTCC blocker, nifedipine (1 μM), confirming the specificity of FPL. Analyzed with one-way ANOVA. * refers to a p value of ≤ 0.02.

4.6 Effects of FST on KCl-induced intracellular calcium rise in WKY and SHR cells

To complement our contractility studies, we wanted to look at the effects of short-term FST treatment on intracellular calcium rise in vascular smooth muscle cells. Using the cell explant technique, I established primary vascular smooth muscle cell cultures in both WKY and SHR. To examine intracellular calcium rise, a fluorescent calcium dye, Fluo-4, was loaded into the cells through a 45-minute incubation at room temperature followed by a 15-minute incubation at 37 °C. Cells treated with FST (500 ng/ml) or nifedipine (1 μM) were incubated with each respective compound for 30 minutes at 37 °C prior to KCl challenge and imaging under the microscope. Shown in Figures 6A and 6B are images pictured at baseline and 120 seconds after adding KCl (125 mM) to WKY control and FST-treated cells as well as SHR control and FST-treated cells, respectively. In Figures 6C and 6D, experimental set-ups of WKY cells were divided into calcium-free and calcium-containing conditions in order to elucidate the effect of FST treatment on calcium entry more directly. In the calcium-free set-up (Figure 6C), cells treated with FST (500 ng/mL) displayed decreased intracellular calcium levels compared to the control and this was similar to cells treated with nifedipine (1 μM). In Figure 6D, when the extracellular media contained calcium, FST and nifedipine-treated cells seemed to be significantly lower in fluorescent signals compared to control cells, suggesting the potential role of FST in blocking intracellular calcium entry. When traces were converted to bar graphs in Figures 6E and 6F, two-way ANOVA statistical analyses revealed no significant differences in intracellular calcium rise

in calcium-free conditions but in calcium-containing media, FST treatment lowered intracellular calcium levels at later time points. The same set-ups were performed in SHR cells and as shown in Figures 6G and 6H, the fluorescent signals observed with FST treatment again closely resemble what is seen with a known, LTCC blocker, nifedipine (1 μM). Figure 6J reveals statistically significant differences in intracellular calcium rise at multiple time points when comparing control and FST-treated cells in calcium-containing media. This suggests a more prominent role of FST in blocking calcium entry in SHR cells compared to WKY cells shown previously (Figure 6F). When comparing Figures 6I and 6J, it is clear that when calcium is present in the extracellular media, FST is able to reduce the entry of the calcium into the cell in SHR cells, as defined by significantly lower fluorescent signals compared to control cells.

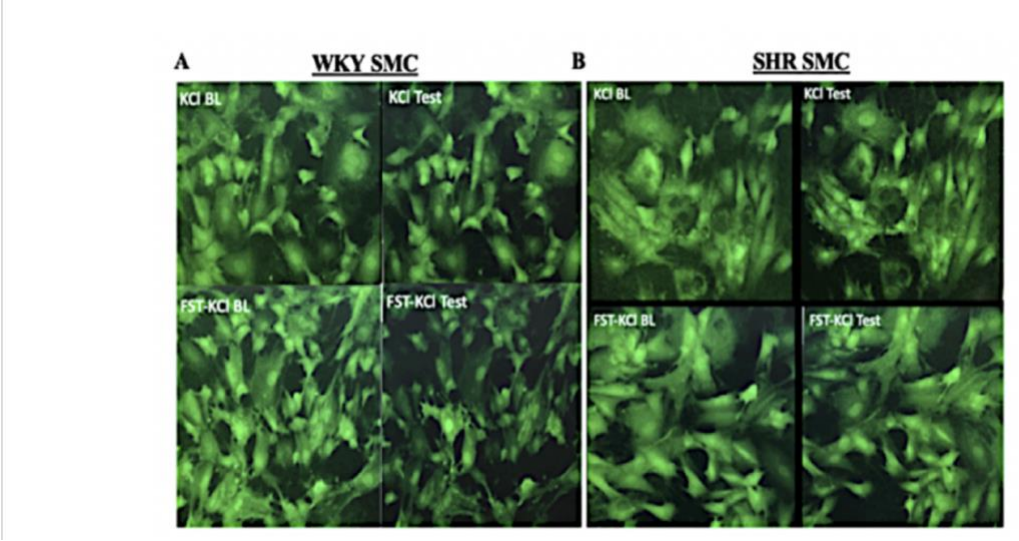
A
WKY SMC
B
SHR SMC
KCl BL
KCl Test
FST-KCl BL
FST-KCl Test
KCl BL
KCl Test
FST-KCl BL
FST-KCl Test

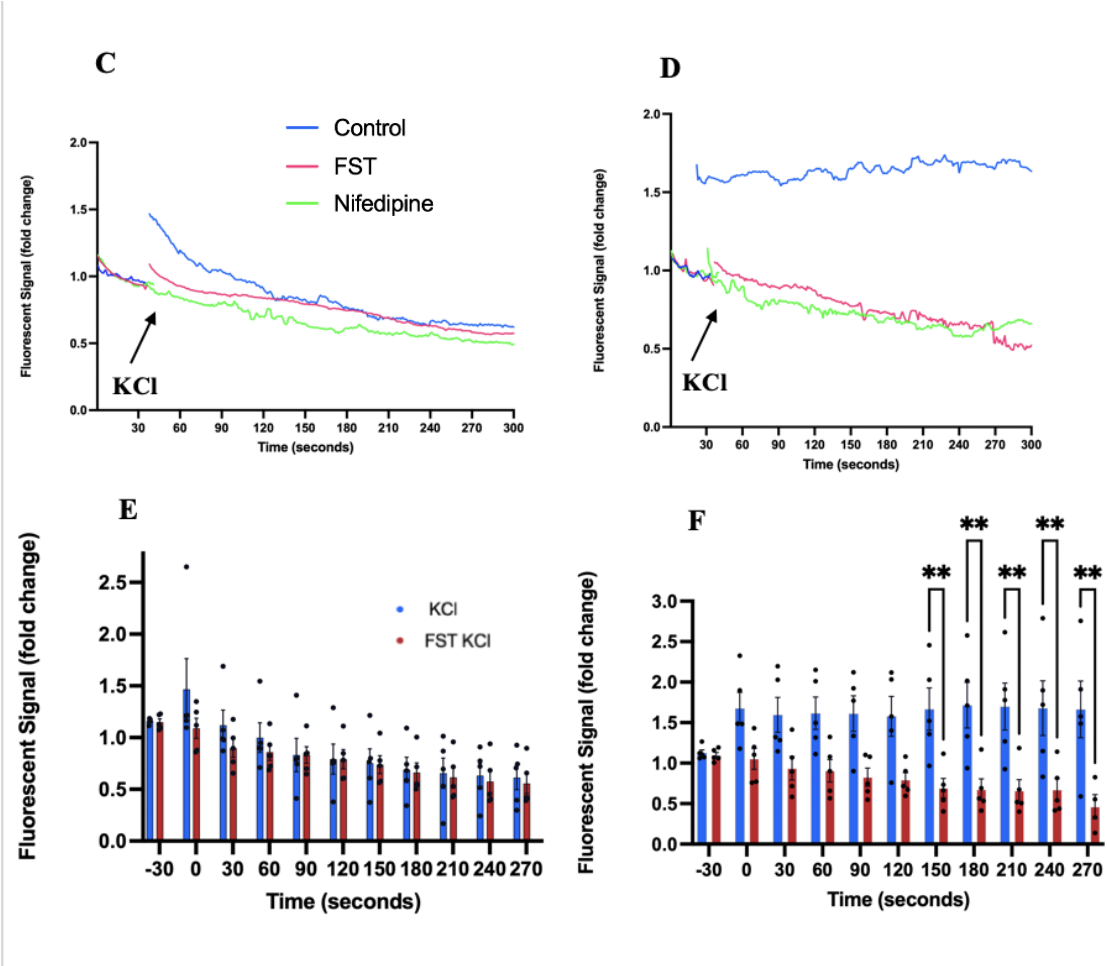
C
Control
FST
Nifedipine
Fluorescent Signal (fold change)
KCl
Time (seconds)
D
Fluorescent Signal (fold change)
KCl
Time (seconds)
E
KCl
FST KCl
Fluorescent Signal (fold change)
Time (seconds)
F
Fluorescent Signal (fold change)
Time (seconds)

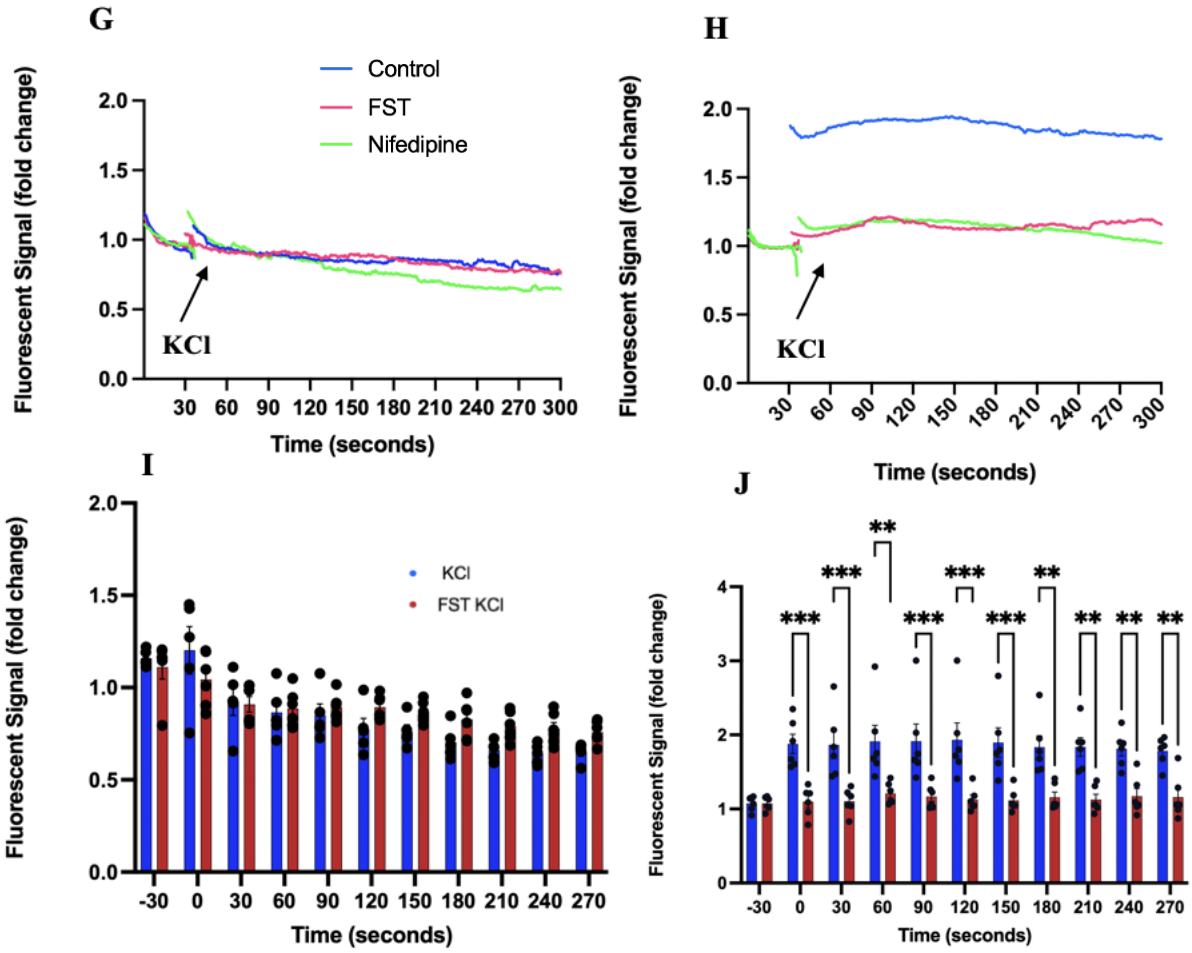

K

[Ca^{2+}] in Control vs FST-treated Cells

	WKY SMC	SHR SMC
Calcium-Free Condition	No significant difference	No significant difference
Calcium-Containing Condition	FST-treated cells significantly ↓ [Ca^{2+}] at later time-points	FST-treated cells significantly ↓ [Ca^{2+}] at almost all time-points

Figure 6. (A) Fluorescent pictures showing WKY control VSMCs or VSMCs treated with FST (500 ng/mL) for 30 minutes, imaged at baseline and upon challenge with KCl (125 mM). (B) Fluorescent pictures showing SHR control VSMCs or VSMCs treated with FST (500 ng/mL) for

30 minutes, imaged at baseline and upon challenge with KCl (125 mM). (C-J) Fluorescent signal measurements from WKY (C-F) and SHR VSMCs (G-J) in either calcium-free (left) or calcium-containing (right) media. Cells were loaded with a calcium indicator dye, fluo-4, treated acutely (30 minutes) with FST (500 ng/mL; red traces), nifedipine (1 μM; green traces) or control media (blue traces), then imaged at baseline and upon challenge with 125 mM KCl through time-lapse imaging. Results show a significant difference in FST-treated WKY cells in calcium-containing medium compared to control cells during the sustained contraction period. FST-treated SHR cells show significant lowering of fluorescent signal at various time points in a calcium-containing medium. (K) Summary diagram of all results. Analyzed with a two-way ANOVA and mixed effects model. (n=4-5). **,*** refers to p values of <0.0095 and <0.0009 respectively.

4.7 Effects of FST intracellular calcium rise induced by lower doses of KCl in SHR cells

We wanted to examine whether lower doses of KCl, as opposed to a maximum dose of 125 mM KCl, induces contraction in our cultured SHR vascular smooth muscle cells. Upon loading of the cells with fluo-4 for 45 minutes at room temperature followed by a 30-minute FST treatment period (500 ng/ml) at 37 °C, cells were challenged with 30 mM KCl or 30 mM NaCl under the microscope. The NaCl group was introduced to allow us to assess the effect of changing the osmotic environment on the signal obtained as it would not be expected to induce as much of a calcium rise compared to KCl. As shown in Figure 7A and 7B, upon KCl challenge, control cells showed approximately a 70% increase in fluorescent signal, indicative of intracellular calcium rise. However, FST pre-treated cells had a significantly decreased signal, suggesting a

reduction of intracellular calcium entry in the presence of FST. The FST-induced reduction in calcium signal was present at almost all time points but was even more significant at earlier time-points. Control cells challenged with 30 mM NaCl had no increased fluorescent response from baseline values.

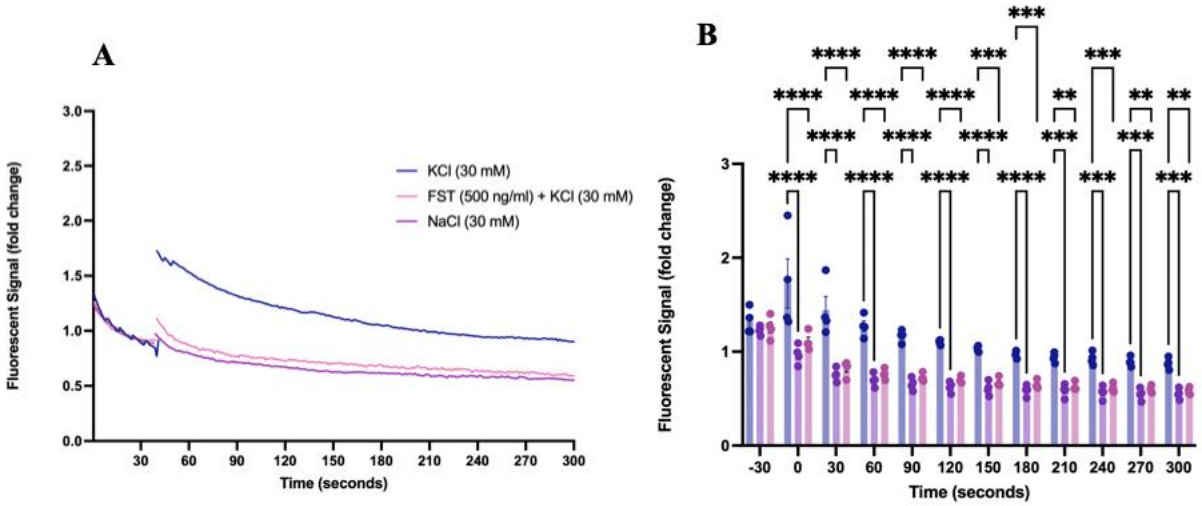

Figure 7. (A,B) Fluorescent signal measurements from SHR cells. Cells were loaded with a calcium indicator dye, fluo-4, treated acutely (30 minutes) with FST (500 ng/mL) then imaged at baseline. Upon challenge with 30 mM KCl or NaCl, time-lapse imaging was completed. Results show FST-treated SHR cells significantly lowering fluorescent signal values at various time points in a calcium-containing medium. Control cells challenged with 30 mM NaCl had no calcium increase. Analyzed with two-way ANOVA. (n=4). **,***,**** refers to p values of <0.002, <0.001 and <0.0001, respectively.

4.8 Presence of LTCC in high passage number SHR cells indicated by nifedipine effects

We wanted to investigate whether later passage cells had decreased expression of LTCCs compared to earlier cell passages. This is because it is known that lines of cells begin to de-differentiate as they are passaged and we wanted to ensure that there was maintained expression of our channel of interest. One of our latest cell passages, which were passage 38-39 cells, were incubated with the Fluo-4 dye for 45 minutes at room temperature prior to a 30-minute treatment period with nifedipine (1 μM) at 37 °C. Cells were then imaged under the microscope and as shown in Figure 8, control cells challenged with 125 mM KCl showed a 50% increase in fluorescent signal, indicative of elevated intracellular calcium rise. Nifedipine-treated cells displayed a reduced fluorescent signal over time, suggesting that nifedipine may be acting on the LTCC to block calcium entry into the SHR cells. Overall, it is apparent that even in late passage cells, nifedipine effects are still present. However, it is important to note that the magnitude of fluorescent signal is higher in earlier passage cells, as shown in Figure 6H when compared to Figure 8. Therefore, earlier passage number vascular smooth muscle cells (P 5-15), as opposed to later ones, have been used for our studies going forward.

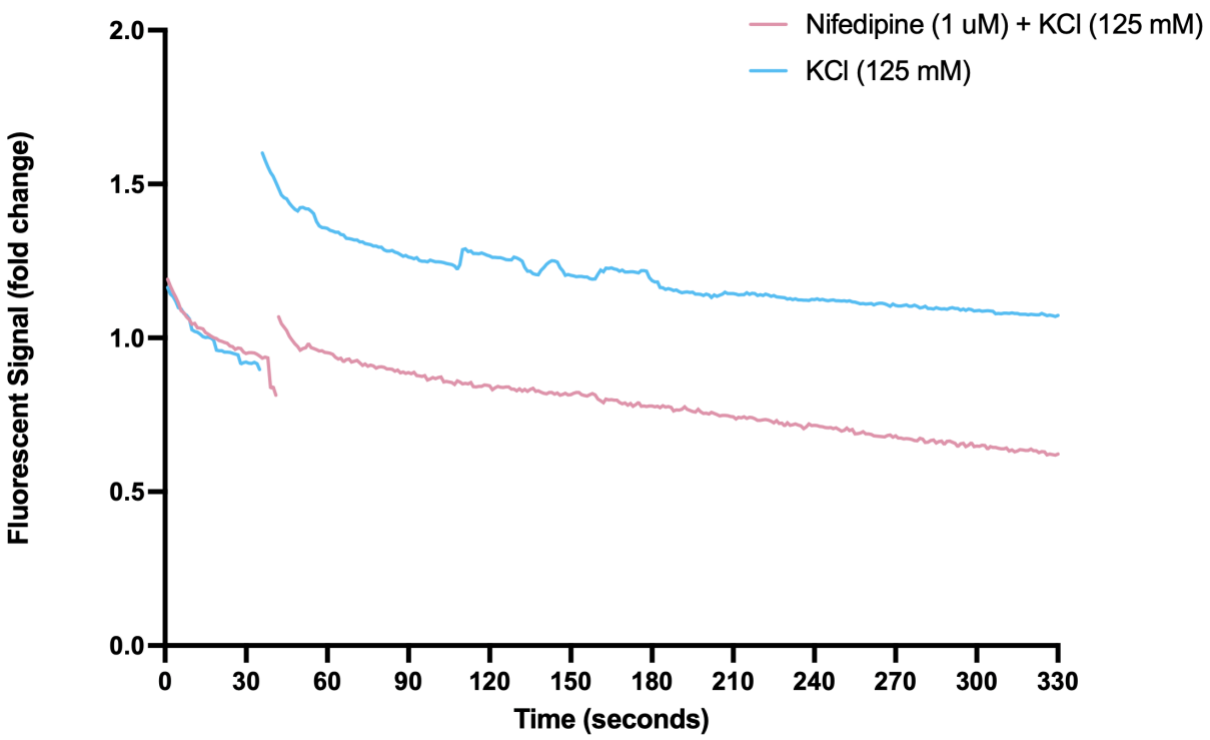

Figure 8. Fluorescent signal measurements from passage 38-39 SHR cells. Cells were loaded with a calcium indicator dye, fluo-4, treated acutely (30 minutes) with nifedipine (1 μM) then imaged at baseline. Upon challenge with 125 mM KCl, time-lapse imaging was completed. Results show nifedipine-treated SHR cells with reduced fluorescent signal values in a calcium-containing medium compared to control cells. Analyzed with Metamorph. (n=2)**.**

4.9 Effects of activin A on intracellular calcium rise in SHR cells

We wanted to examine whether short-term treatment of our SHR vascular smooth muscle cells with activin A (50 ng/ml) would affect the KCl-induced calcium rise. Since the contractility experiments done in Figure 2 showed an elevation of KCl-induced contraction with activin A treatment, we wanted to see if the same augmentation in signal would be present in cells. Upon loading of the cells with Fluo-4 for 45 minutes at room temperature followed by a 30-minute activin A treatment period (50 ng/ml) or control media incubation at 37 °C, cells were challenged with 125 mM KCl or distilled water (dH_2O) under the microscope. As shown in Figure 9A and 9B, upon KCl challenge, activin-A treated cells showed approximately a 2.5-fold increase in fluorescent signal that was statistically significant at multiple time points compared to control cells stimulated with 125 mM KCl, indicative of augmented intracellular calcium rise. Control cells stimulated with dH_2O had a blunted response that wavered at baseline values, suggesting no calcium rise.

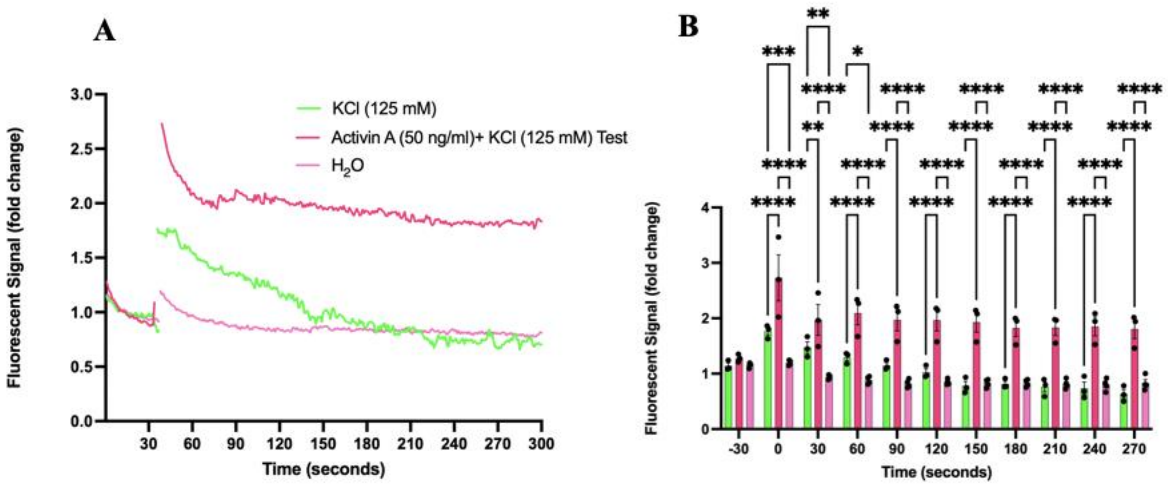

Figure 9. (A,B) Fluorescent signal measurements from SHR VSMCs loaded with a calcium indicator dye, Fluo-4, treated acutely (30 minutes) with activin A (50 ng/ml) or control media then imaged at baseline and upon challenge with 125 mM KCl; time-lapse imaging was completed. Results show a significantly augmented increase in intracellular calcium in the activin A-treated cells challenged with KCl compared to control cells while the dH_2O-stimulated cells showed no increase in signal. Analyzed with two-way ANOVA. (n=3-4). *,**,***,**** refers to p values of <0.03, <0.009, <0.0007, <0.0001 and respectively.

4.10 Effects of shorter imaging frequency on Activin A augmentation of KCl-induced intracellular calcium rise in SHR cells

We wanted to investigate whether a shorter total imaging time and reduced imaging frequency would affect the rise then early drop in signal observed with activin A-augmentation of KCl-induced calcium rise over time (shown in Figure 9) . Upon loading of the cells with the Fluo-

4 dye for 45 minutes at room temperature followed by a 30-minute activin A treatment period (50 ng/ml) or control media incubation at 37 °C, cells were challenged with 125 mM KCl or dH_2O under the microscope. As shown in Figure 10A and 10B, activin A pre-treatment (50 ng/ml) significantly augmented the increased calcium signal caused by KCl (125 mM) while dH_2O stimulation had no effect on either control cells or cells pre-treated with activin A (50 ng/ml). It is clear that reduced imaging frequency and total imaging time have beneficial effects in increasing the magnitude of fluorescent signal when comparing the signals obtained with the same treatment groups in Figure 9. Additionally, the drop in signal in the Activin-A treated cells challenged with KCl is more gradual, rather than steep, throughout the imaging period. Activin A-treated cells challenged with KCl (125 mM) show a 3-fold increase in fluorescent signal, indicative of augmented calcium rise (Figure 10). This signal drops down and stabilizes at the 2.5-fold increase in signal mark for the remainder of the imaging period (100 seconds). Control cells challenged with KCl (125 mM) show a 1.5-fold increase in signal that is relatively stable throughout the entire imaging period.

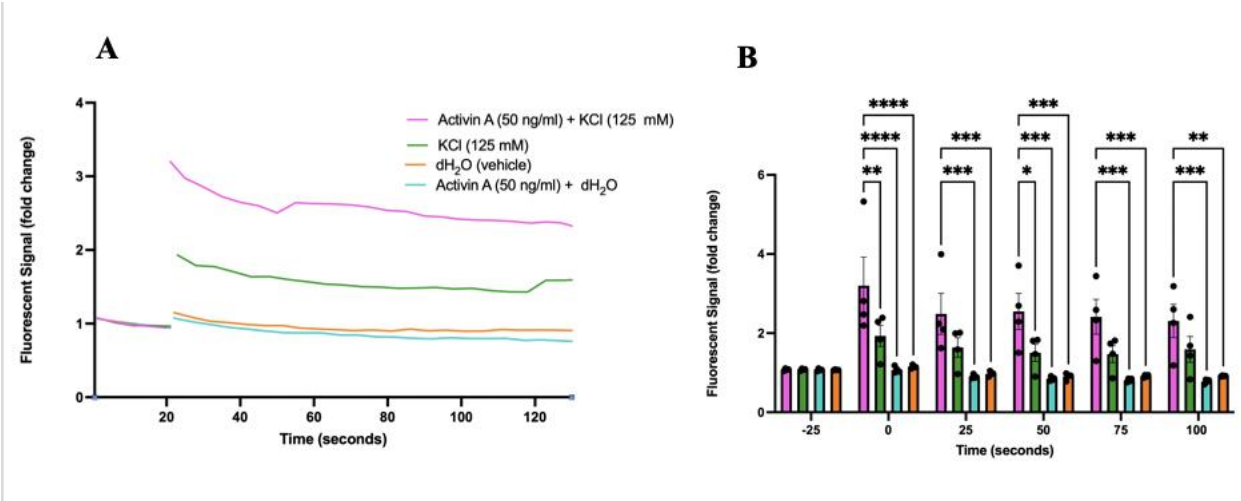

Figure 10. (A,B) Fluorescent signal measurements from SHR VSMCs loaded with a calcium indicator dye, Fluo-4, treated acutely (30 minutes) with activin A (50 ng/ml) or control media then imaged at baseline and upon challenge with 125 mM KCl or stimulation with dH_2O; time-lapse imaging was completed for a duration of 2 minutes (1 frame/5 seconds). Results show a stable and significantly augmented increase in intracellular calcium in the activin A-treated cells challenged with KCl compared to control cells while the dH_2O-stimulated cells showed no increase in signal. Analyzed with two-way ANOVA (n=4). *,**,***,**** refers to p values of <0.04, <0.007, ≤ 0.0009 and <0.0001, respectively.

4.11 Examining osmotic effects on intracellular calcium rise in SHR cells

We wanted to test whether the KCl-induced increase in fluorescent signal, indicative of calcium rise, was not solely due to osmotic effects. Following the loading of the cells with Fluo-4 for 45 minutes at room temperature, cells were incubated in control media at 37°C and then challenged with either KCl (125 mM), dH_2O or mannitol (250 mM) under the microscope. As shown in Figure 11A and 11B, cells challenged with KCl (125 mM) displayed an approximate 50% increase in fluorescent signal while the cells stimulated with mannitol (250 mM) and dH_2O had minimal rise in response. When comparing the KCl group with mannitol, there was a statistically significant increase in calcium signal with KCl, especially in the first 90 seconds of the imaging period. There was no statistically significant difference between the mannitol and dH_2O group, suggesting that the initial rise in signal observed upon cell stimulation is present in some treatment groups, regardless of its osmolarity. However, distinct treatment groups do differ in the magnitude of initial rise observed.

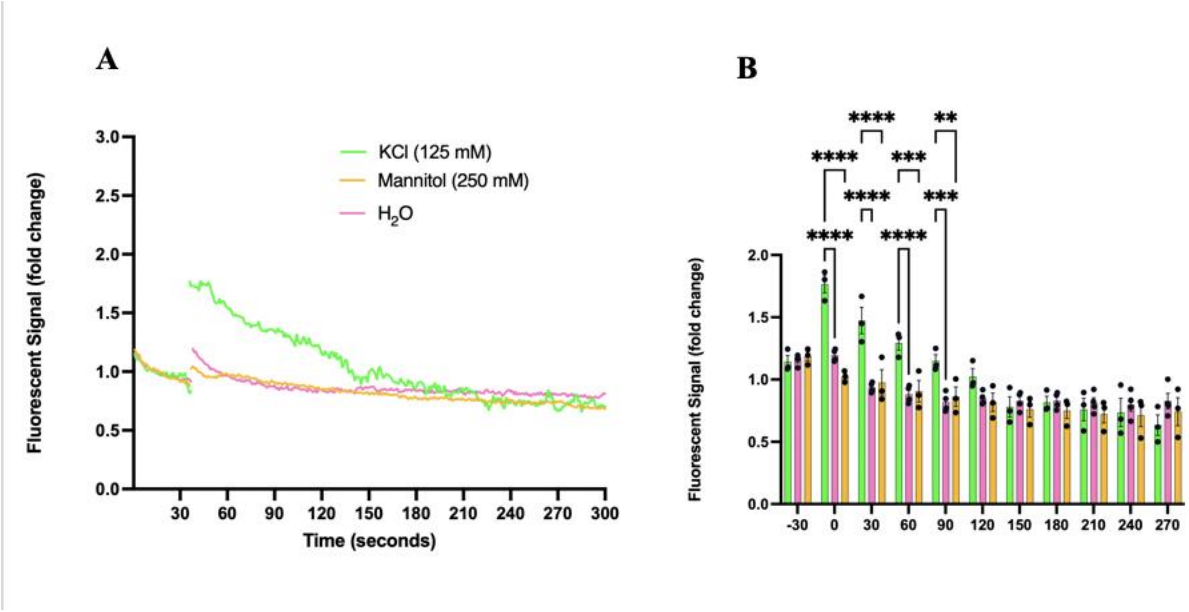

Figure 11. (A,B) Fluorescent signal measurements from SHR VSMCs loaded with a calcium indicator dye, Fluo-4, incubated in control media then imaged at baseline and upon challenge with 125 mM KCl, 250 mM mannitol or stimulation with dH_2O; time-lapse imaging was done. Results show a significant increase in calcium signal with control cells challenged with KCl compared to control cells stimulated with either mannitol or dH_2O at all time points until the 90 second mark of the imaging period. Analyzed with two-way ANOVA (n=3-4). **,***, **** refers to p values of <0.007, ≤0.0007 and <0.0001 respectively.

4.12 Investigating the role of intracellular calcium stores on activin A effects

We wanted to further investigate the mechanism through which short-term activin A (50 ng/ml) treatment of SHR vascular smooth muscle cells augmented KCl-induced calcium rise. To do this, we used thapsigargin, an inhibitor of the endoplasmic reticulum calcium ATPase, in order to create a condition where intracellular calcium stores are disrupted. Following the loading of cells with Fluo-4 for 45 minutes at room temperature, cells were treated with activin A (50 ng/ml), thapsigargin (200 nM) or control media for 30 minutes at 37 °C. Cells were then challenged with 125 mM KCl under the microscope. As shown in Figure 12A and 12B and as observed previously, upon KCl challenge, Activin-A treated cells show approximately a 2.5-fold increase in fluorescent signal that drops down to a 2-fold increase in signal over time. Thapsigargin and Activin-A treated cells show a similar response to cells treated with activin A alone, as there is no statistically significant difference between the two groups, except the first two time-points of the imaging period. Control cells challenged with KCl (125 mM) displayed a 1.5-fold increase while cells pre-treated with thapsigargin and challenged with KCl (125 mM) showed an initial augmented calcium rise but this was not statistically significant. Therefore, even when intracellular calcium stores were disrupted with thapsigargin treatment, activin A still augmented the KCl-induced calcium rise, suggesting that activin A effects on mediating calcium levels are dependent on extracellular calcium.

To further corroborate the finding that activin A may be exerting its calcium effects extracellularly, cells were placed in a calcium-free media during pre-treatment with either activin A (50 ng/ml) or media alone. As shown in Figure 12C and 12D, both control cells and activin A (50 ng/ml) pre-treated cells challenged with KCl (125 mM) had an initial rise in signal that was quickly dropped throughout the remainder of the imaging period, indicating minimal activin A or

KCl effects in the absence of extracellular calcium. Since the same rise in signal was present in cells that were stimulated with a non-stimulating solution such as Ca^{2+}-free HBSS, the initial rise then drop in signal observed with KCl stimulation in Ca^{2+}-free conditions could be due to an artifact. Lastly, control cells stimulated with calcium-free HBSS had a similar initial rise in signal to the other groups.

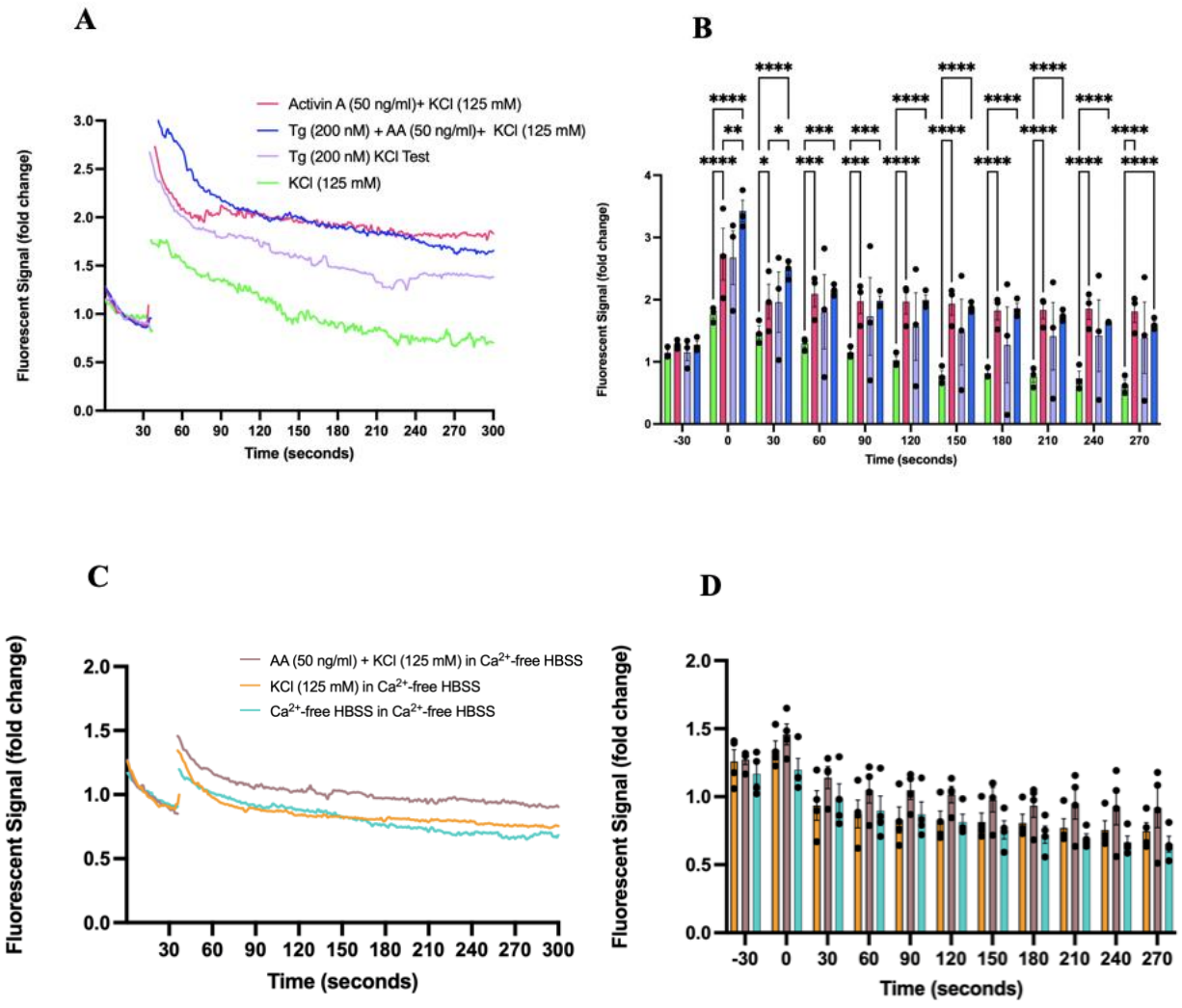

Figure 12. (A,B) Fluorescent signal measurements from SHR VSMCs loaded with a calcium indicator dye, Fluo-4, treated either with activin A (50 ng/ml) and thapsigargin (200 nM) together, alone or in control media then imaged at baseline. Upon challenge with 125 mM KCl, time-lapse imaging was done. Results show a similarly significant increase in calcium signal with activin A-treated cells and cells treated with activin A and thapsigargin together when challenged with KCl. (C,D) Both control cells and activin A pre-treated cells placed in a calcium-free media and challenged with either KCl (125 mM) or calcium-free HBSS displayed a similar initial rise in signal that decreased over time. Analyzed with two-way ANOVA (n=3-4). *,**,***,**** refers to p values of <0.04, <0.003, ≤ 0.0004 and <0.0001, respectively.

4.13 Examining the effects of activin neutralization on intracellular calcium rise in SHR cells

In order to conduct contractility experimental set-ups in parallel with cell studies, we used the Fluo-4 calcium dye to also repeat the anti-activin experiment shown in Figure 1. The fluorescent signals shown as traces in Figure 13A reveal increased intracellular calcium in SHR cells upon the addition of KCl (125 mM) when cells were treated with mouse IgG1 (3.5 µg/ml) and a neutralizing Activin B antibody (3.5 µg/ml) but not in cells treated with a neutralizing activin A antibody (3.5 µg/ml) for 30 minutes. When traces were converted to bar graphs to allow for statistical analysis (Figure 13B), it was shown that at all time points, the neutralization of activin A but not activin B reduced intracellular calcium levels in SHR cells.

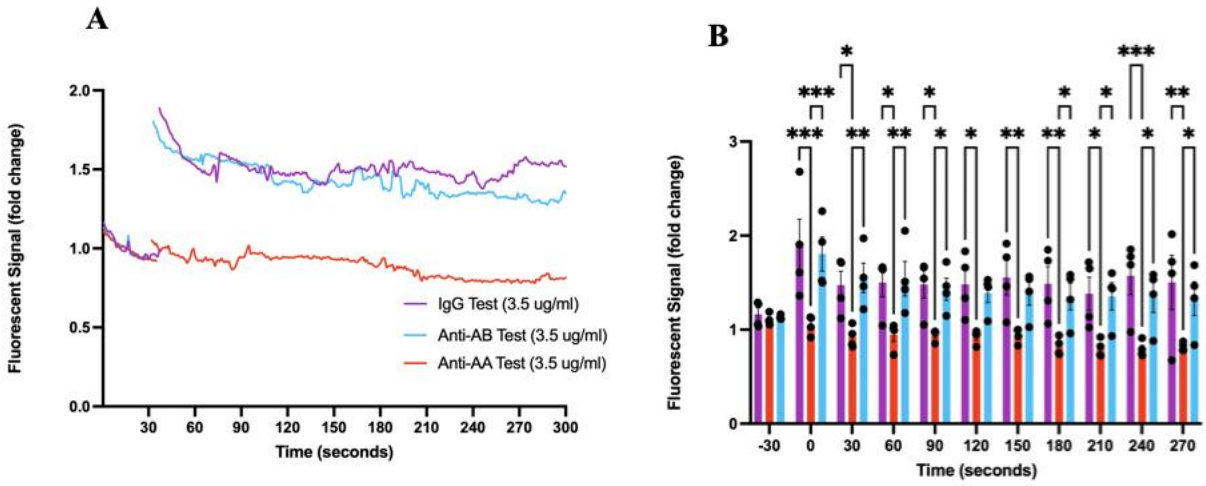

Figure 13. (A,B) Fluorescent signal measurements from SHR VSMCs loaded with a calcium indicator dye, Fluo-4, treated acutely (30 minutes) with mouse IgG1 (3.5 µg/ml), a neutralizing activin A antibody (3.5 µg/ml) and a neutralizing activin B antibody (3.5 µg/ml) for 30 minutes then imaged at baseline. Upon challenge with 125 mM KCl, time-lapse imaging was done. Results show a significant decrease in intracellular calcium in the anti-activin A group compared to the IgG control and anti-activin B treated VSMCs. Analyzed with a two-way ANOVA. (n=4). *,**,*** refers to p values of <0.005, <0.008 and ≤0.0008 respectively.

4.14 Effects of direct activin A stimulation on intracellular calcium and potassium levels in SHR cells

We wanted to examine whether activin A could induce a rise in intracellular calcium in the absence of KCl. Following the loading of cells with Fluo-4 for 45 minutes at room temperature, cells were incubated in control media for 30 minutes at 37 °C. Cells were then challenged directly with either activin A (50 ng/ml) or activin A buffer under the microscope and imaged for a duration of 2 minutes (1 frame/second). As shown in Figure 14A and 14B, although both groups displayed an initial, subtle rise in signal, this was not stable and reduced dramatically for the duration of the imaging period. The differences in fluorescent signal between the cells stimulated with activin A and activin A buffer were minimal and not statistically significant.

With the aim of tracking intracellular potassium levels, we also used a fluorescent potassium indicator, IPG-1 AM. Compared with other potassium indicators, IPG-1 AM has a relatively low affinity to potassium, allowing for better detection of small changes in potassium levels of the cell with the benefit of minimizing excess background noise. Specifically, we wanted to see whether direct activin A stimulation could affect intracellular potassium levels in the absence of KCl. Following the loading of cells with IPG-1 for 1 hour at 37 °C, cells were challenged directly with either activin A (50 ng/ml) or activin A buffer under the microscope and imaged for a duration of 2 minutes (1 frame/second). As shown in Figure 14C and 14D, both groups showed an initial, miniscule rise in fluorescent signal but this was only present in the first few seconds of imaging and then was reduced for the remainder of the two-minute imaging period. There was no statistically significant difference in the fluorescent potassium signals of cells stimulated with either activin A or activin A buffer at all time-points. Lastly, we wanted to further explore whether activin A could induce a rise in intracellular calcium in the absence of

KCl through a long-term imaging period. Upon loading of cells with Fluo-4 for 45 minutes at room temperature, cells were incubated in control media for 30 minutes at 37 °C. Cells were then challenged directly with either activin A (50 ng/ml) or activin A buffer under the microscope and imaged for a duration of 15 minutes (1 frame/10 seconds). As shown in Figure 14E and 14F, both groups showcased a small rise in signal upon stimulation but the signal decreased and remained low for the duration of the imaging period. There was no statistically significant difference in fluorescent signals between the cells stimulated with activin A and activin A buffer at any time-point.

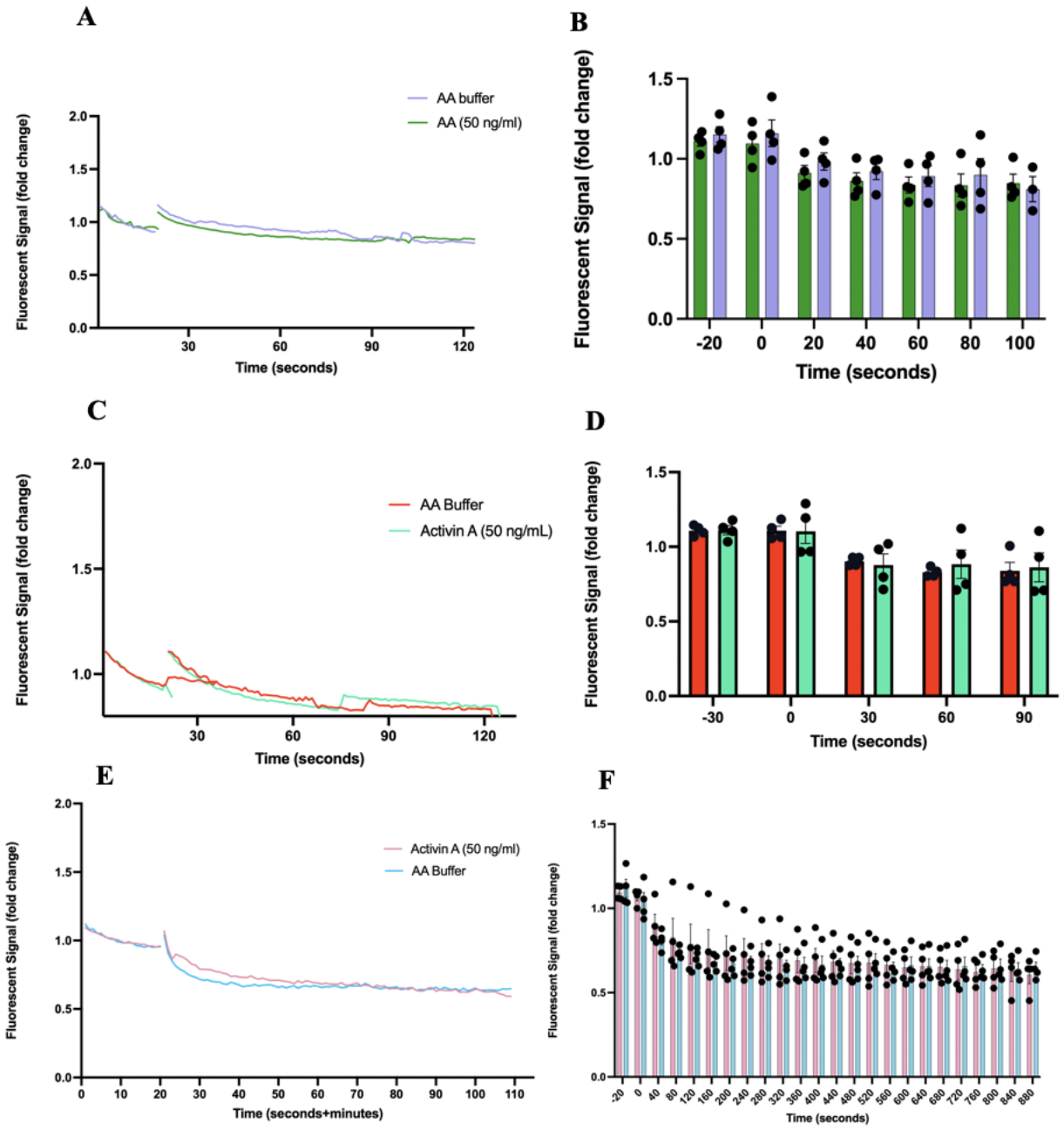

Figure 14. (A,B) Fluorescent signal measurements from SHR VSMCs loaded with a calcium indicator dye, Fluo-4, incubated in control media then imaged at baseline. Upon challenge with activin A (50 ng/ml) or activin A buffer, time-lapse imaging was done for a duration of 2 minutes (1 frame/second). Results show a minimal increase in calcium signal that was present with both

groups and which was not statistically significant at any time-point. (C, D) Fluorescent signal measurements from SHR VSMCs loaded with a potassium indicator dye, IPG-1, then imaged at baseline prior to stimulation with activin A (50 ng/ml) or activin A buffer. Time-lapse imaging was then completed for a duration of 2 minutes (1 frame/ second). Results show a small, initial rise in fluorescent signal upon stimulation with both treatment groups which was not statistically significant at any time-point. (E, F) Fluorescent signal measurements from SHR VSMCs loaded with calcium indicator dye, Fluo-4, incubated in control media then imaged at baseline. Upon challenge with activin A (50 ng/ml) or activin A buffer, time-lapse imaging was done for a duration of 15 minutes (1 frame/10 seconds). Results show a minute, initial rise in signal with both groups which decreased over time and which was not significantly different from one another at any time-point. Analyzed with two-way ANOVA (n=4).

4.15 Effects of varying doses of KCl on intracellular potassium rise in SHR cells

We wanted to examine if short-term FST treatment affected intracellular potassium levels upon stimulation with KCl**.** Initially, we performed a KCl dose-response on SHR cells loaded with IPG-1 AM for 1 hour at at 37 °C to determine which KCl dose would be optimal for use in FST studies. As shown in Figure 15A, images represent control cells in HBSS at baseline and upon the addition of HBSS during the test phase as well as cells at baseline and challenged with 42 mM, 84 mM or 125 mM KCl. Figures 15B and 15C show increased intracellular potassium levels in response to KCl doses, with the greatest signal increase being with the 125 mM KCl dose. Upon statistical analysis, no significant difference in fluorescent signal was found between

the 84 mM and 125 mM doses, with the latter being chosen for ensuing IPG-1 experiments in order to stay consistent with the KCl dose used in previous calcium and potassium assay experiments. In Figure 15C, cells were either treated with control media or FST (500 ng/mL) for 30 minutes at 37 °C. Figures 15C and 15D reveal a large difference in intracellular potassium levels upon KCl challenge (125 mM) in control cells compared to FST-treated cells. This suggests that FST does something to inhibit the rise in intracellular potassium triggered by KCl, whether this may be through the prevention of potassium influx into the cell or increasing the leak of potassium out of the cell.

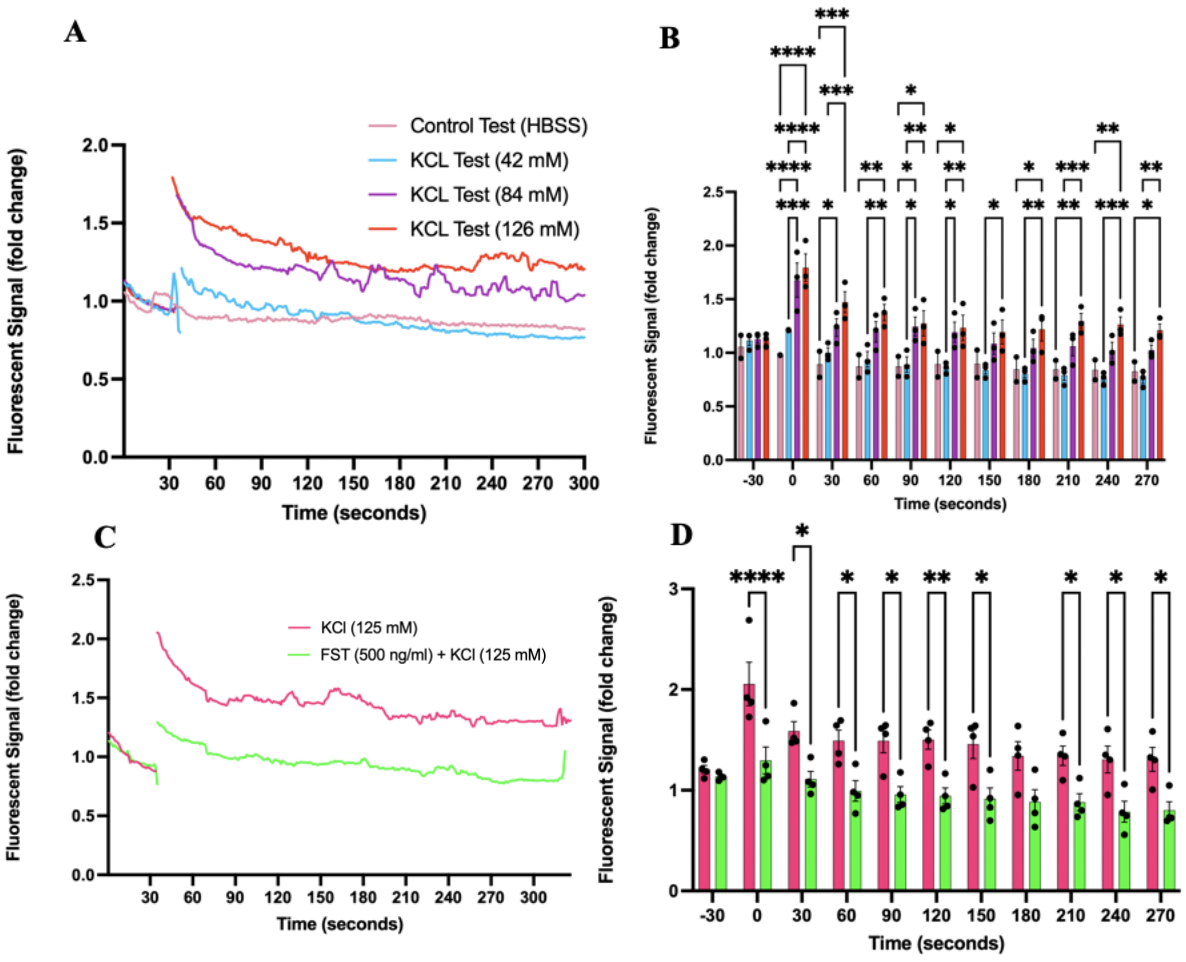

Figure 15. (A,B) Fluorescent signal measurements from SHR VSMCs loaded with potassium indicator dye, IPG-1 AM, challenged with KCl (42 mM, 84 mM, 125 mM) and imaged through time-lapse imaging. Results show an increased signal with the 84 mM and 125 mM KCl doses compared to cells receiving the 42 mM dose and negative control cells. Analyzed with two-way ANOVA (n=4) *,**,***,**** refers to p values of <0.02, <0.002, <0.0009 and <0.0001, respectively. (C,D) Fluorescent signal measurements from SHR VSMCs loaded with potassium indicator dye, IPG-1 AM, treated acutely (30 minutes) with FST (500 ng/mL) then challenged with KCl (125 mM) and imaged. Results show significantly increased intracellular potassium levels in control cells compared to FST-incubated cells upon the KCl (125 mM) challenge. Analyzed with two-way ANOVA (n=4). *,**,***,**** refers to p values of <0.05, <0.0095, ≤0.0007 and <0.0001, respectively.

4.16 Effects of activin A on intracellular potassium rise in response to KCl in SHR cells

We wanted to examine whether, similar to the results obtained from the Fluo-4 calcium assays, whether activin A would affect intracellular potassium levels. SHR cells were loaded with the fluorescent potassium indicator, IPG-1 for 1 hour at 37 °C prior to being treated in control media or with activin A (50 ng/ml) for an additional 30 minutes at 37 °C. Following this, cells were imaged under the microscope for a baseline period, challenged with KCl (125 mM) then imaged through time-lapse imaging. As observed in Figure 16A and 16B, both control cells and cells pre-treated with activin A displayed a similar rise in fluorescent signal, indicative of intracellular potassium entry, upon KCl stimulation. There was no statistically significant

difference in the signal observed between control cells and activin A cells, suggesting that activin A does not augment KCl-induced intracellular potassium entry.

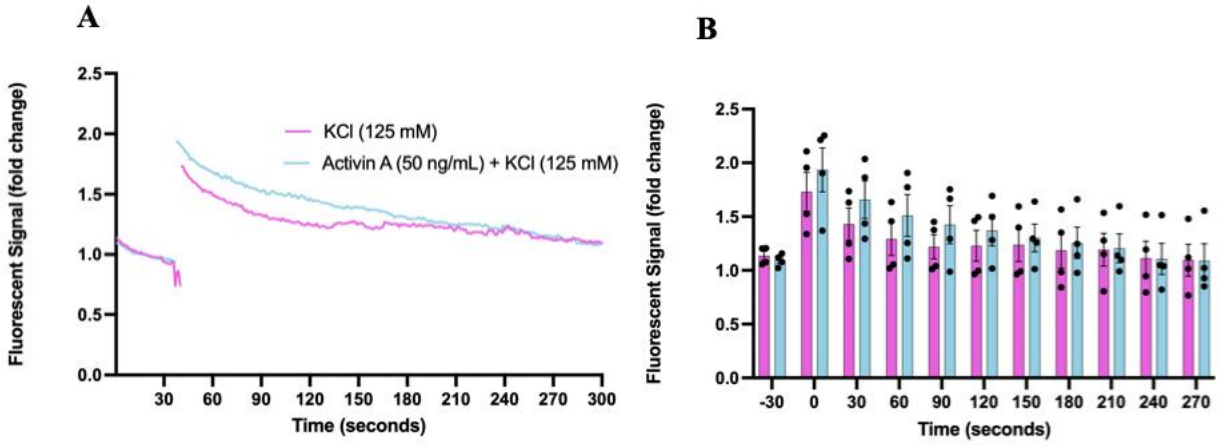

Figure 16. (A,B) Fluorescent signal measurements from SHR VSMCs loaded with potassium indicator dye, IPG-1 AM, treated with activin A (50 ng/ml) or in control media, imaged at baseline, challenged with KCl (125 mM) then imaged. Results show a similarly increased signal with both treatment groups that have no statistically significant differences at any time-point. Analyzed with two-way ANOVA. (n=4).

4.17 Effects of activin neutralization on intracellular potassium rise in response to KCl in SHR cells

We wanted to investigate whether the neutralization of either activin A or activin B with neutralizing antibodies had any effect on intracellular potassium entry and determine if FST effects on reducing intracellular potassium may have been activin-mediated. SHR cells were loaded with the fluorescent potassium indicator, IPG-1 for 1 hour at 37 °C prior to being treated with mouse IgG1 (3.5 µg/ml), a neutralizing activin A antibody (3.5 µg/ml) and a neutralizing activin B antibody (3.5 µg/ml) for an additional 30 minutes at 37 °C. Following this, cells were imaged under the microscope for a baseline period, challenged with KCl (125 mM) then imaged. As observed in Figure 17A and 17B, cells treated with the activin A neutralizing antibody displayed lower fluorescent signals, indicative of reduced intracellular potassium in response to the KCl challenge, when compared to the IgG and anti-activin B treated cells. This difference was statistically significant at multiple time-points. The fluorescent signals obtained with the IgG and anti-activin B groups were similar throughout the full duration of the imaging period and both displayed an approximate 2-fold increase in fluorescence from baseline values. This suggests that the neutralization of potential basal activin A levels in SHR cells may contribute to the reduction of KCl-induced calcium rise.

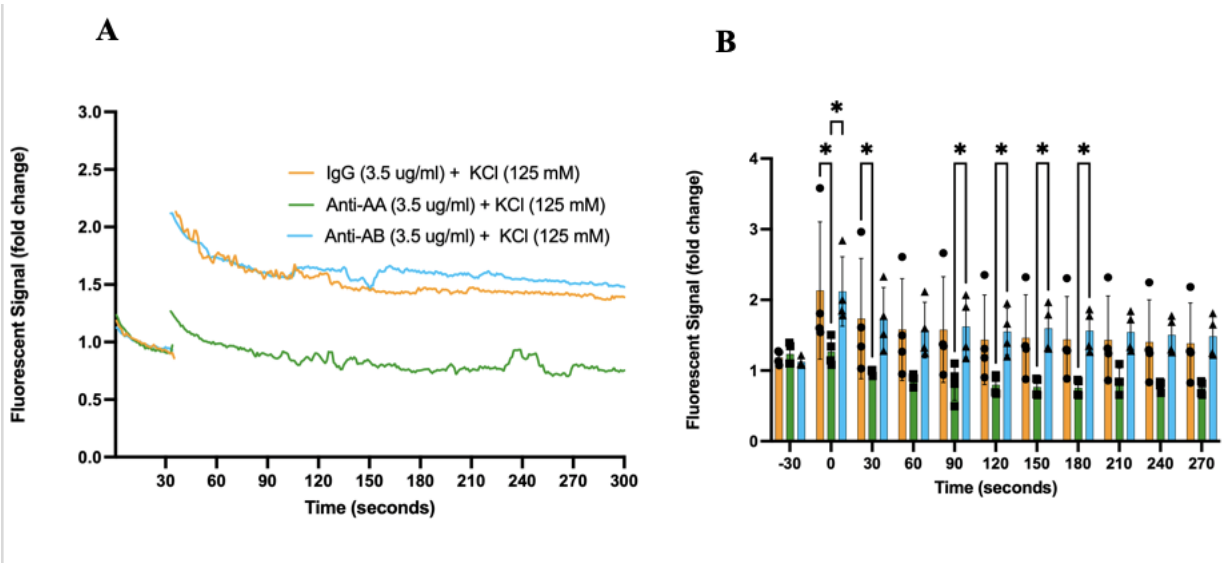

Figure 17. (A,B) Fluorescent signal measurements from SHR VSMCs loaded with a potassium indicator dye, IPG-1, treated with mouse IgG1 (3.5 µg/ml), a neutralizing activin A antibody (3.5 µg/ml) and a neutralizing activin B antibody (3.5 µg/ml) for 30 minutes then imaged at baseline. Upon challenge with 125 mM KCl, time-lapse imaging was completed). Results show a significant and similar rise in intracellular potassium in the IgG and anti-activin B group from baseline and compared to the anti-activin A treated VSMCs which had significantly lowered fluorescent signal. Analyzed with a two-way ANOVA. (n=4). * refers to a p value of <0.05.

4.18 Direct effects of FST on basal membrane potential in SHR cells

We wanted to examine whether direct FST stimulation would affect membrane potential as assessed by the potential sensitive dye, $DiBAC_4(3)$. Following the loading of cells with the $DiBAC_4(3)$ dye for 30 minutes at 37 °C, cells were challenged directly with either FST (500 ng/ml) or HHBSS under the microscope and imaged for a duration of 20 minutes (1 frame/minute). As shown in Figure 18A and 18B, both groups did not display any rise in signal throughout the imaging period. More specifically, the fluorescent signal wavered and was not statistically significant between cells stimulated with either FST or HBSS at any time point. Therefore, FST does not seem to have any acute effect on membrane potential measurements.

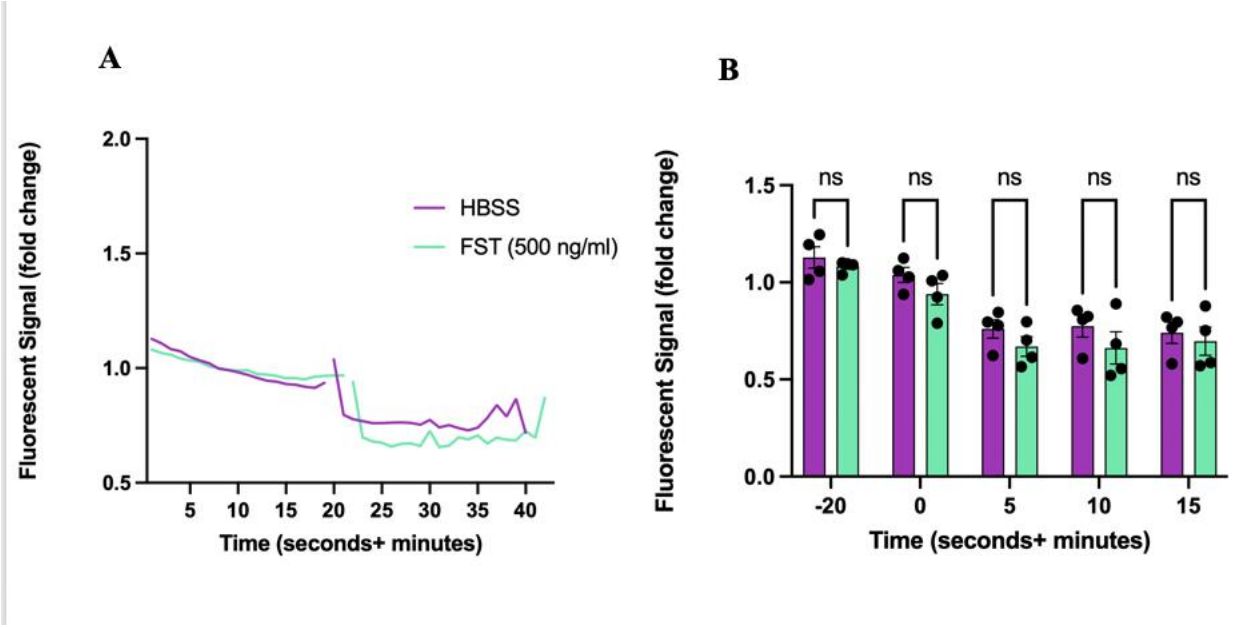

Figure 18. (A,B) Fluorescent signal measurements from SHR VSMCs loaded with a membrane potential sensitive probe, $DiBAC_4(3)$, then imaged at baseline prior to stimulation with FST (500 ng/ml) or HBSS. Time-lapse imaging was then completed for a duration of 20 minutes (1 frame/minute). Results show no increase in fluorescent signal upon stimulation with either

treatment groups and this was not statistically significant at any time-point. Analyzed with two-way ANOVA (n=4).

4.19 Effects of FST treatment on KCl-induced membrane potential changes in SHR cells

We wanted to then investigate whether FST pre-treatment would affect membrane potential changes caused by KCl (125 mM) stimulation using the same potential sensitive dye, $DiBAC_4(3)$. During the loading of cells with the $DiBAC_4(3)$ dye, select wells were also treated with FST (500 ng/ml) for 30 minutes at 37 °C. Cells were then challenged with KCl (125 mM) under the microscope and imaged for a duration of 2 minutes (1 frame/5 seconds). As shown in Figure 19A and 19B, control cells challenged with KCl displayed an approximate 1.5-fold increase in fluorescent signal, indicative of depolarization, compared to baseline values. Furthermore, FST-treated cells had a much lower rise in signal upon KCl challenge and this reduced signal remained stable throughout the imaging period. Control cells had a significantly higher fluorescent signal at all time-points in comparison to FST-treated cells.

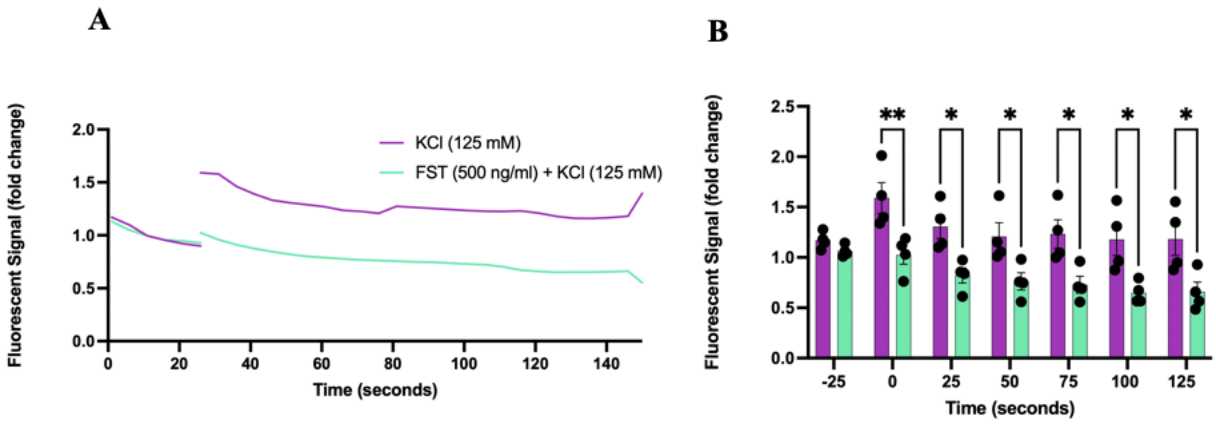

Figure 19. (A,B) Fluorescent signal measurements from SHR VSMCs loaded with a membrane potential sensitive probe, $DiBAC_4(3)$, treated with FST (500 ng/ml) or incubated in control media then imaged at baseline prior to stimulation with KCl (125 mM). Time-lapse imaging was then completed for a duration of 2 minutes (1 frame/5 seconds). Results show an increase in fluorescent signal upon stimulation with KCl that was significantly higher in control cells. Analyzed with two-way ANOVA (n=4). *,** refers to p values of <0.05 and 0.0055, respectively.

4.20 Potential photobleaching effects present with increased imaging frequency in SHR cells

As observed in Figure 20A, some of our initial KCl challenge experiments carried out with the $DiBAC_4(3)$ dye had a reduction of signal over time, which was present even in our control cells. In these experiments, upon loading of cells with the $DiBAC_4(3)$ dye for 30 minutes at 37 °C, cells were challenged with KCl (125 mM) and imaged for a duration of 6 minutes at an imaging frequency of 1 frame/second. In order to troubleshoot the concern with a diminishing fluorescent signal, we wanted to examine whether this could be due to potential photobleaching from a high imaging frequency and a relatively long imaging time. As shown in Figure 20B, upon KCl challenge of both control cells and cells pre-treated acutely (30 minutes) with FST (500 ng/ml), there was an approximate 1.5-fold increase in fluorescence, initially, which was being reduced over time. The imaging was then paused for a brief 3-4 minute period prior to resuming the experiment. It is clear that when the imaging was continued, there was a recovery and stabilization in the diminishing fluorescent signal. In Figure 20C, SHR control cells are shown at 20X magnification prior to imaging as well as at 10X magnification following an imaging period

of 120 seconds at an imaging frequency of 1 frame/second. Three cells were selected and quantified for their fluorescent signals at both 20X and 10X following imaging and the results showed a statistically significant decrease in fluorescence. However, it is important to note that the selected cells did not display a decrease in signal in the central area of view, characteristic of photobleaching. Therefore, photobleaching may be taking place, but its effects are subtle as there are no morphological changes induced in the cells.

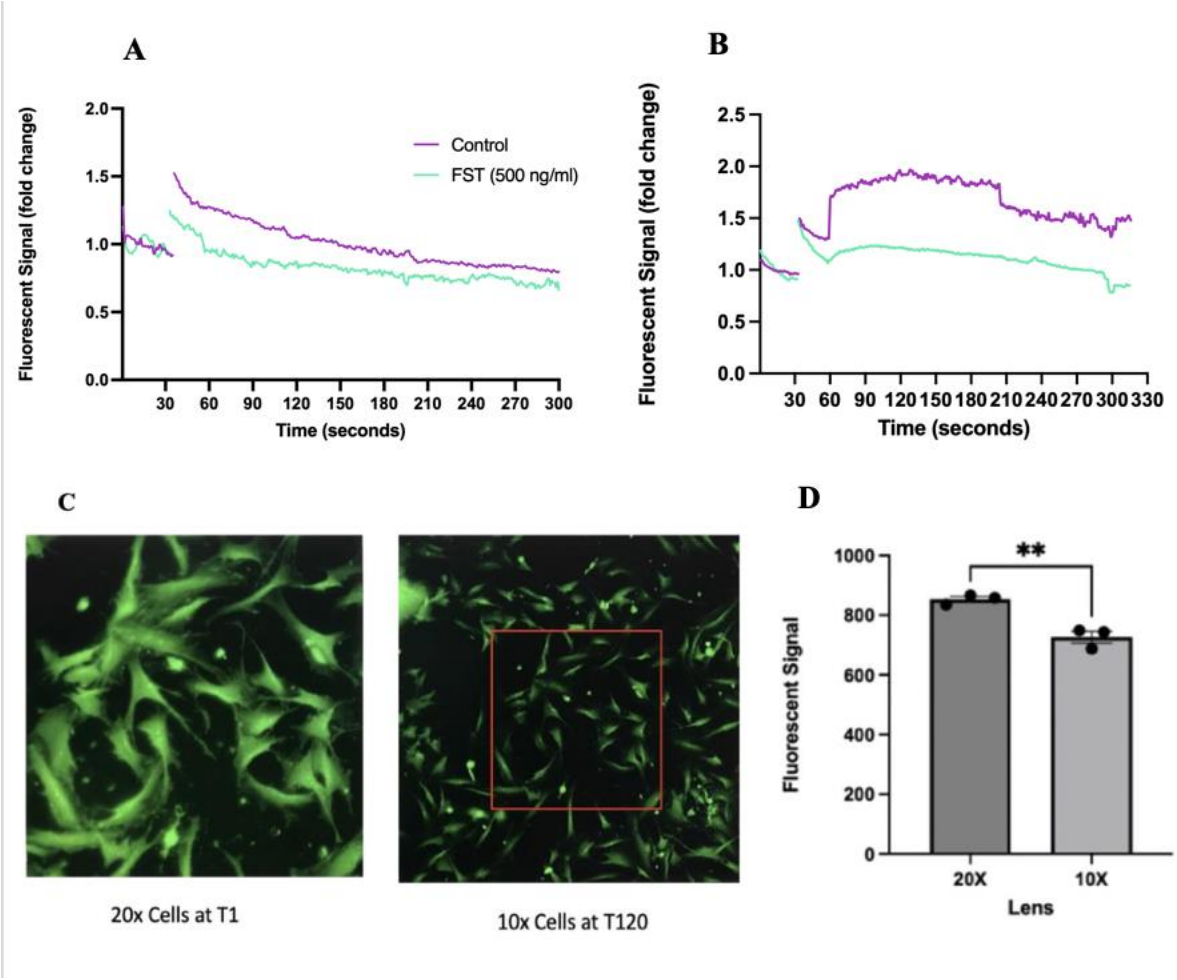

Figure 20. (A) Fluorescent signal measurements from SHR VSMCs loaded with a membrane potential sensitive probe, $DiBAC_4(3)$, treated with FST (500 ng/ml) or incubated in control media then imaged at baseline prior to stimulation with KCl (125 mM). Time-lapse imaging was then completed for a duration of 6 minutes (1 frame/second). Results show an increase in fluorescent signal upon stimulation with KCl that quickly diminishes over time (n=4) (B) When imaging was paused at T=60 seconds for 3-4 minutes and then resumed, the diminished signal began to recover and plateaued over time (n=1) (C) Cells imaged at 20X magnification then at 10X magnification following a 2-minute imaging period (T120) had a statistically significant reduction in signal but displayed no morphological changes. Analyzed with unpaired t-test (n=3). ** refers to a p value of 0.043.

4.21 Effects of FST and activin neutralization on phenylephrine- induced contraction *in SHR vessels*

To explore whether FST effects are generalizable to agonists other than KCl, both SHR control and FST pre-treated vessels (500 ng/ml) mounted onto the myograph were challenged with increasing doses of another contractile agent, phenylephrine (10^{-8} to 10^{-4} M). As shown in Figure 21A, control vessels had an elevated contractile response compared to FST vessels, and this was statistically significant at the higher doses ($10^{-5.5}$ to $10^{-4.5}$ M). The effects of FST on lowering contraction were therefore present even in response to phenylephrine as the agonist. In Figure 21B, we wanted to study whether the FST effects observed in Figure 9A were activin-mediated. Vessels that were treated with a neutralizing activin A antibody (3.5 µg/ml) had significantly lower phenylephrine-induced contraction compared to vessels treated with mouse

IgG1 (3.5 µg/ml) or an activin B neutralizing antibody (3.5 µg/ml) at doses $10^{-5.5}$ M and doses $10^{-5.5}$ to 10^{-5} M, respectively. When anti-activin A vessels were compared to FST vessels, there was no significant difference in their contractile response to phenylephrine, as shown in Figure 21A, suggesting that the observed FST effects in reducing vessel contraction may be activin-mediated. Specifically, FST may be exerting its effects through the neutralization of activin A.

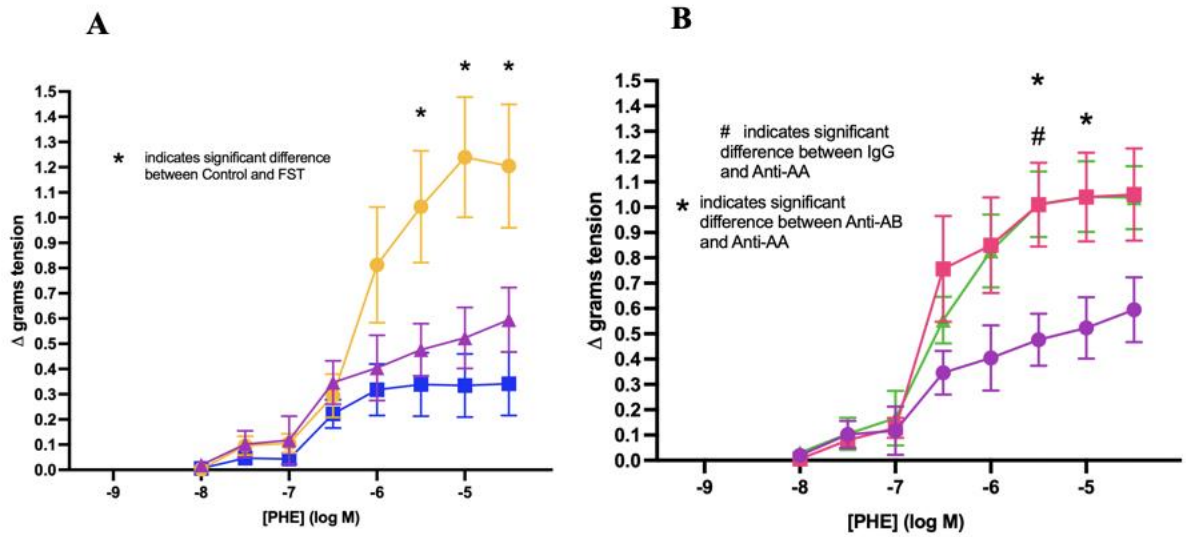

Figure 21. Contractility measurements shown in gram tension values from 30-week-old SHR (A) Control vessels challenged with increasing doses of phenylephrine (10^{-8} to 10^{-4} M) displayed a significantly increased contraction compared to vessels treated acutely (30 minutes) with FST (500 ng/ml) at phenylephrine doses of $10^{-5.5}$ to $10^{-4.5}$ M. There was no significant difference in contractile responses of FST vessels and vessels pre-treated with a neutralizing activin A antibody (3.5 µg/ml) (B) SHR vessels treated with a neutralizing activin A antibody (3.5 µg/ml) had a significantly reduced contractile response compared to vessels treated with mouse IgG1 (3.5

µg/ml) or a neutralizing activin B antibody (3.5 µg/ml) at doses $10^{-5.5}$ to 10^{-5} M. Analyzed with unpaired multiple t-tests. (n=4). *, # refer to p-values of <0.04.

4.22 Effects of FST and Activin Neutralization on 5-HT- induced contraction *in SHR vessels*

To further explore whether FST effects are generalizable to agonists other than KCl, both SHR control and FST pre-treated vessels (500 ng/ml) were stimulated with increasing doses of a potent vasoconstrictor, serotonin (5-hydroxytryptamine; 5-HT), at a dose range of 10^{-8} to 10^{-4} M. As shown in Figure 22A, control SHR vessels had an increased contractile response compared to FST pre-treated vessels, which was statistically significant at the higher doses of $10^{-5.5}$ to $10^{-4.5}$ M. This shows that the effects of FST in reducing contraction were existent with 5-HT as the constrictor, similar to what was observed with phenylephrine as the agonist. In Figure 22B, we wanted to study whether the FST effects in lowering 5-HT induced contraction were activin-mediated. Vessels pre-treated with a neutralizing activin A antibody (3.5 µg/ml) had significantly reduced 5-HT-induced contraction compared to vessels treated with mouse IgG1 (3.5 µg/ml) at doses of $10^{-5.5}$ and $10^{-4.5}$ M. When the contractile response of anti-activin A vessels were compared to vessels pre-treated with an activin B neutralizing antibody (3.5 µg/ml), it was shown that the neutralization of activin A significantly reduced 5-HT contraction in the dose range of 10^{-6} to $10^{-4.5}$ M. As shown in Figure 22A, there was no significant difference in the contractile response of FST vessels and anti-activin A vessels to 5-HT.

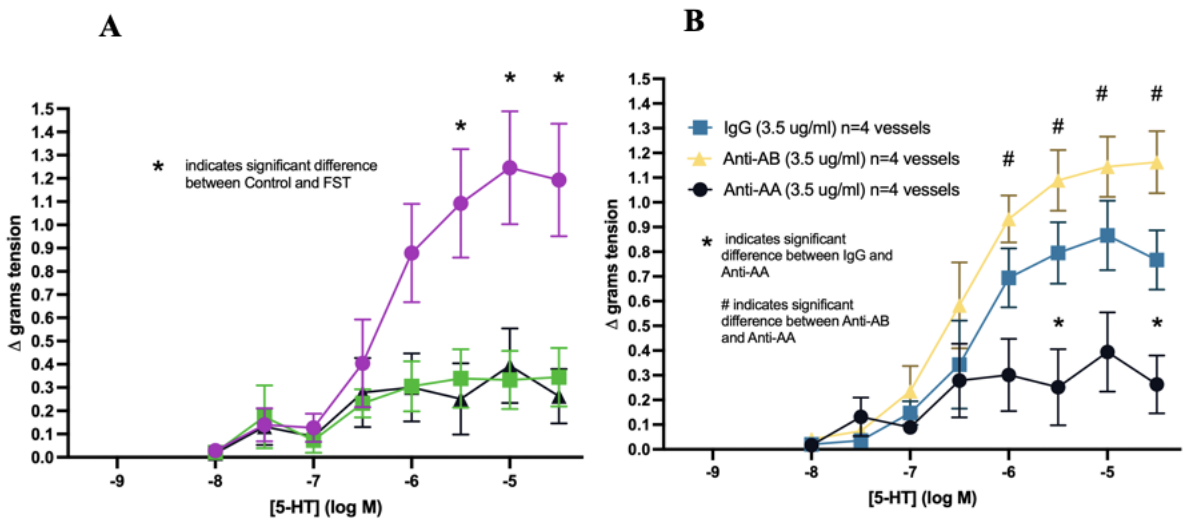

Figure 22. Contractility measurements shown in gram tension values from 30-week-old SHR (A) Control vessels challenged with increasing doses of 5-HT (10^{-8} to 10^{-4} M) displayed a significantly increased contraction compared to vessels treated acutely (30 minutes) with FST (500 ng/ml) at 5-HT doses of $10^{-5.5}$ to $10^{-4.5}$ M. There was no significant difference in contractile responses of FST vessels and vessels pre-treated with a neutralizing activin A antibody (3.5 µg/ml) (B) SHR vessels treated with a neutralizing activin A antibody (3.5 µg/ml) had a significantly reduced contraction compared to vessels treated with mouse IgG1 (3.5 µg/ml) at doses $10^{-5.5}$ and $10^{-4.5}$ M or at doses 10^{-6} to $10^{-4.5}$ M when compared to vessels pre-treated with a neutralizing activin B antibody (3.5 µg/ml). Analyzed with multiple unpaired t-tests. (n=4). * refers to p-values of <0.04 and # refers to p-values of <0.01, respectively.

4.23 Effects of FST on angiotensin II-induced contraction *in SHR vessels*

To determine whether FST effects were generalizable to agonists other than KCl, contractility studies using Angiotensin II were performed. First, a dose-response to angiotensin II (10^{-8} to 10^{-6} M) was performed on SHR vessels to determine the optimal dose for use with FST. As shown in Figure 23A, vessels challenged with the 10^{-7} M angiotensin II dose elicited the greatest contraction and were used for angiotensin II studies going forward. Vessels were incubated in either control media or FST (500 ng/mL) for 30 minutes prior to mounting for wire myography. In Figure 23B, no significant difference was observed between control vessels and FST-treated vessels challenged with 10^{-7} M angiotensin II. However, it is important to note that the contraction obtained with angiotensin II, even in control vessels, was lower than what is typically elicited with agonists such as KCl, phenylephrine and serotonin, as shown previously. The lower strength of contraction in control vessels could be a reason why there is no significant difference between control and FST pre-treated vessels.

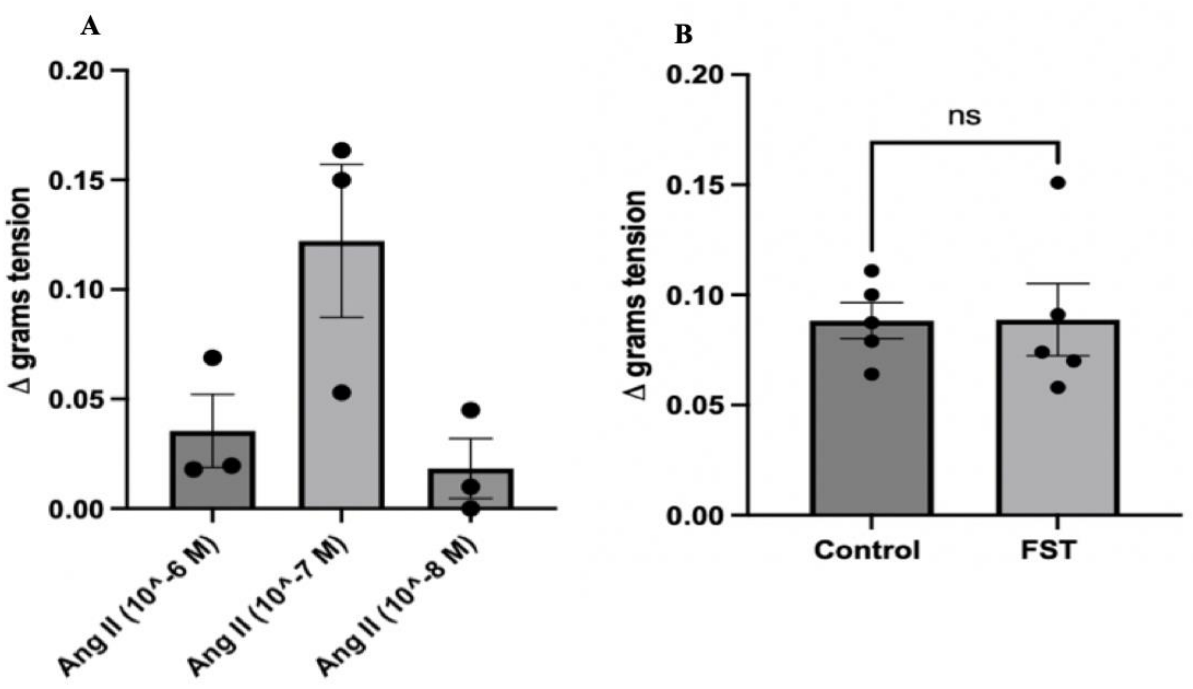

Figure 23. Contractility measurements shown in gram tension values from 30-week-old SHR (A) vessels acutely challenged with increasing doses of angiotensin II (10^{-8} to 10^{-6} M) show increased contraction with the greatest contraction elicited from the 10^{-7} M angiotensin II dose (B) SHR vessels treated acutely with FST (500 ng/mL) showed similar, non-significant differences in contraction with 10^{-7} M angiotensin II compared to control vessels. Analyzed with one-way ANOVA.

4.24 Effects of FST on Smad3 activating phosphorylation

In order to examine the effects of short-term FST treatment on activin signalling molecules, immunohistochemistry studies were performed on WKY and SHR vessels incubated either in control media or with FST (500 ng/mL) for 30 minutes at 37 °C prior to fixing, processing, embedding and sectioning. As shown in Figure 24B, pSMAD3 is significantly elevated in SHR control vessels compared to WKY control vessels. FST-treated SHR vessels show a significant reduction in pSMAD3 compared to SHR control vessels. This suggests the potential role of FST in hindering basal activin signalling.

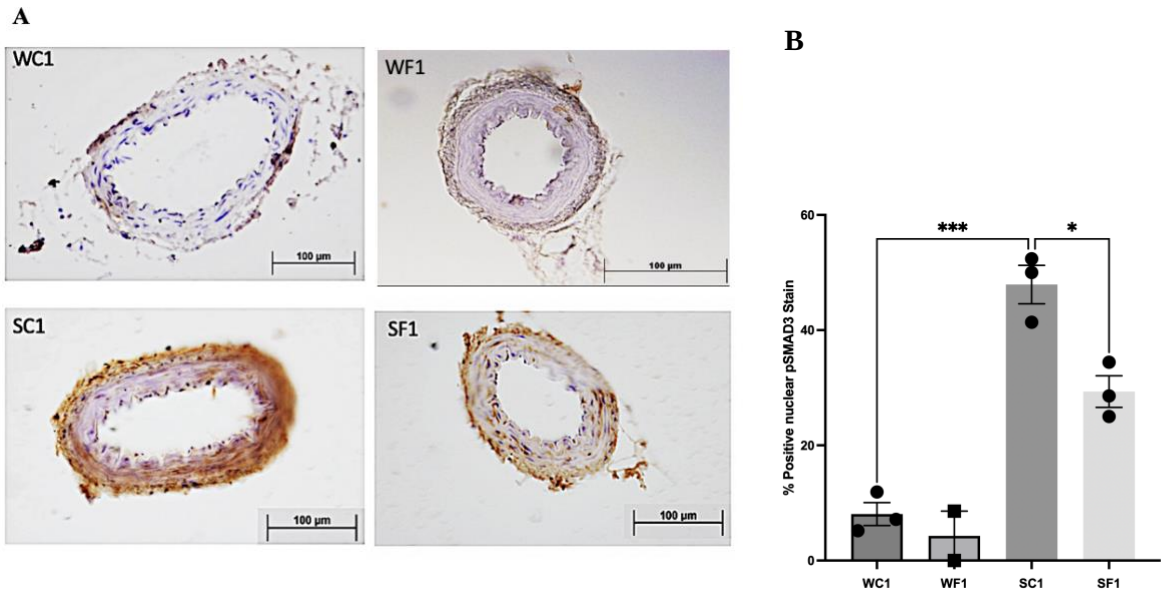

Figure 24. Immunohistochemistry studies done on 30-week-old WKY and SHR vessels acutely incubated (30 minutes) with FST (500 ng/mL) or control media, then fixed in 4% PFA show increased nuclear staining in SHR control vessels compared to WKY vessels which is

significantly reduced by short-term FST treatment. Analyzed with one-way ANOVA. (n=2-3). * and *** refers to p values of <0.0011 and 0.0001 respectively.

4.25 Effects of contractile agonists on MYPT phosphorylation in the medial layer of SHR vessels

We wanted to explore the effects of various agonist treatments on the phosphorylation of the contractile protein, MYPT, in SHR vessels. Immunohistochemistry studies were carried out on SHR vessels incubated either in control media for 30 minutes, activin A (50 ng/ml) for 30 minutes, angiotensin II (1 µM) for 10 minutes or KCl (125 mM) for 5 minutes at 37 °C prior to fixing, processing, embedding and sectioning. As shown in Figure 25, p-MYPT staining in the medial layer of vessels is more significantly elevated in the SHR vessels treated acutely with KCl (125 mM) relative to the other treatment groups and in comparison to SHR control vessels. This is indicative of a prominent role of KCl in regulating contraction by increasing the levels of p-MYPT in vascular smooth muscle cells of SHR vessels.

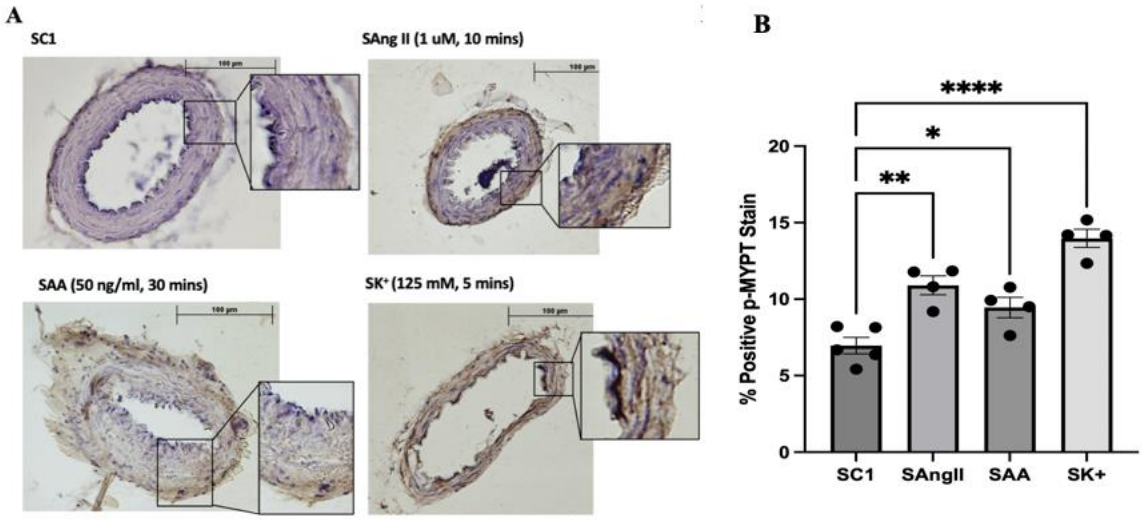

Figure 25. Immunohistochemistry studies done on 30-week-old WKY and SHR vessels incubated (30 minutes) with activin A (50 ng/mL) or control media, angiotensin II (1 µM) for 10 minutes or KCl (125 mM) for 5 minutes then fixed in 4% PFA show elevated p-MYPT staining in SHR KCl-treated vessels compared to control SHR vessels. Analyzed with one-way ANOVA. (n=4-5). *,** and **** refers to p values of <0.05, <0.002, and <0.0001, respectively.

4.26 Summary Model

As observed through our experimental data, FST may be reducing KCl-induced contraction via various mechanisms. One main possibility includes the closing of the LTCC, which would reduce calcium influx in the VSMC, thereby inhibiting contraction. FST may act directly on the LTCC or exert its effects indirectly through the neutralization of activin A. Experiments conducted with the neutralizing activin antibodies suggest that the latter case is more likely. FST may also contribute to the opening of the K-ATP channel, stimulating potassium efflux and consequentially, smooth muscle relaxation. As shown through the agonist generalizability contractility experiments, it is clear that FST may also reduce vessel contraction induced by GPCR-agonist stimuli such as phenylephrine and 5-HT. A study done by Paulis et al. has shown that nifedipine was able to partially block norepinephrine stimulation of SHR vessels, to a greater degree than in WKY vessels [85]. This finding suggest that FST could potentially reduce contraction caused by both KCl and GPCR-mediated stimulation via a similar action on the LTCC.

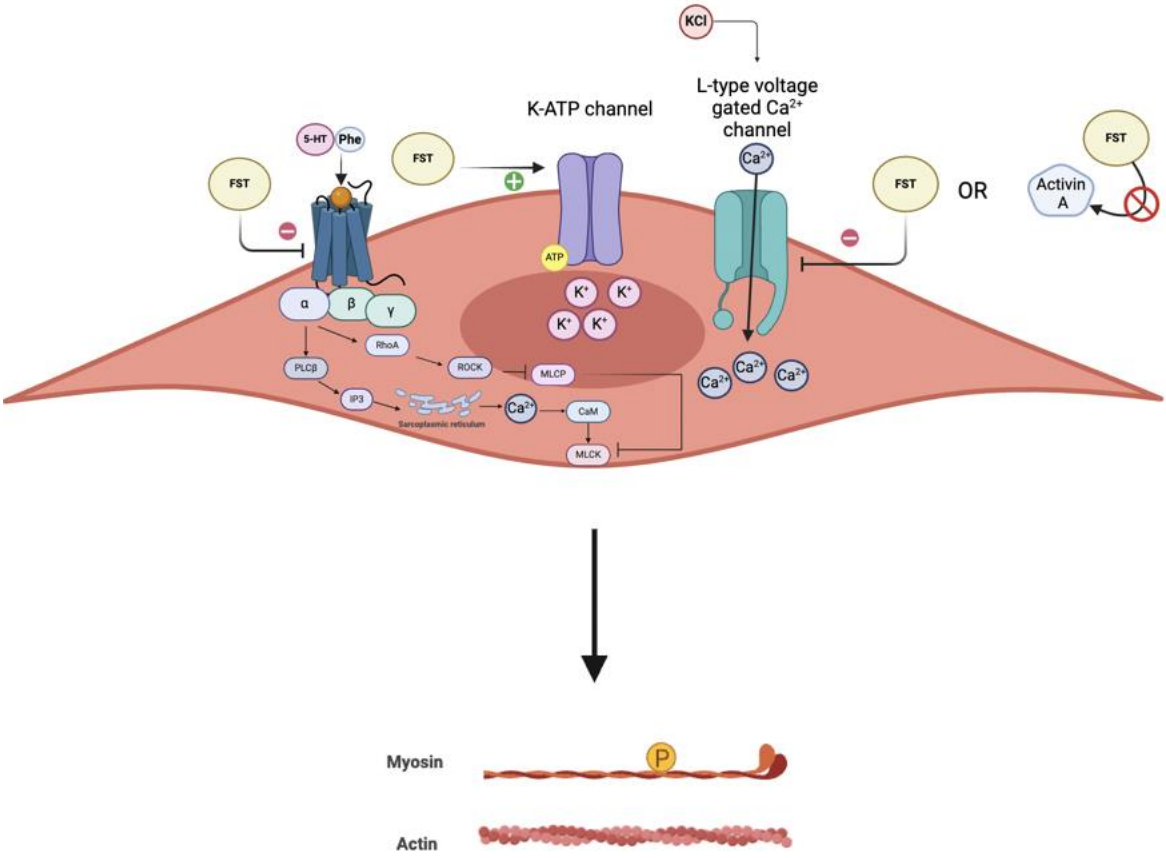

Vascular Smooth Muscle Cell Contraction

Discussion

As HTN is the leading cause of death worldwide and over 245,700 people in Canada suffer from resistant HTN, there is always a need to develop novel therapeutic agents [1, 76]. Our work in illustrating the mechanisms through which FST, a potential anti-hypertensive agent, may be working to reduce vessel contraction, is significant in aiding drug development and optimization. It is likely that FST, through neutralization of activin A, as opposed to activin B, is reducing KCl-induced contraction in part by acting to decrease calcium influx in SHR cells. Activin A seems to augment calcium influx by acting on smooth muscle entry of extracellular calcium, potentially through LTCCs, rather than intracellular calcium stores as shown in Figure 12. Additionally, FST mediates potassium influx in SHR cells and is likely through activin A neutralization. However, this is less conclusive as activin A pre-treatment did not affect potassium levels in SHR cells.

Our results thus far have shown that FST mediates its contraction-lowering effects through the neutralization of activin A, as opposed to activin B (Figure 1). The contribution of activin A to KCl-induced constriction also seems to be more pronounced in SHR vessels compared to normotensive WKY vessels as shown in our activin neutralization studies (Figure 1). It is also important to note that when comparing the calcium assays in WKY smooth muscle cells compared to SHR cells, FST reduces calcium influx at many more time points in the SHR than in the WKY cells (Figure 6). This difference could be explained by the 3.4-fold increased expression of LTCC subunit (α_{1C}) in SHR mesenteric arteries compared to WKY [63]. However, it is also likely that the early passage SHR cells (Passage 3) used in these initial experiments were more resistant to potential photobleaching or dye extrusion compared to WKY cells, which would

explain their resistance to signal drop over time in calcium-containing conditions. Our activin neutralization findings have also been supported through calcium and potassium assays where short-term treatment of SHR vascular smooth muscle cells with the same neutralizing antibodies used in our contractility studies caused a similar lowering of calcium influx and intracellular potassium levels to FST with neutralization of activin A but not activin B (Figure 13, 17). When vessels were treated with activin A (Figure 2), SHR vessels displayed augmented potassium-induced contractility, further supporting that activin A plays a more prominent role in the contraction of SHR vessels, which FST can mediate through neutralization.

It was also clear that activin receptor inhibition reduced potassium-induced vessel contraction to a similar degree as FST in both WKY and SHR vessels (Figure 3). However, the use of a TGF-β neutralizing Ab (1 μg/mL) in SHR vessels did not reduce potassium-induced contraction. This suggests that short-term FST treatment is likely to reduce KCl- contraction primarily through inhibition of activin signalling, but not through TGF-β signalling. A study conducted by Yndestad et al. has found elevated activin A levels in patients with pulmonary HTN. Yndestad et al. have also shown increased TGF-β activity, demonstrated as increased Smad 2/3 phosphorylation despite unchanged pulmonary activin A levels, in lungs of mice with pulmonary HTN induced by subjecting mice to hypoxia for 2 weeks, which highlights a potential role of TGF-β in HTN pathophysiology [78]. Our lack of relevant TGF-β findings could be due to the relatively short treatment period (30 minutes) of our SHR vessels, which may not be sufficient to induce transcriptional changes mediated by TGF-β that could potentially alter vessel contractility measurements.

On a cellular basis, activin A pre-treatment of SHR cells augmented the KCl-induced rise in intracellular calcium compared to untreated cells, as observed through Fluo-4 calcium assays

(Figure 12). The results of a study conducted by Takano et al. has also shown that direct activin A stimulation of pituitary adenoma cells significantly increased calcium influx [52]. Various other studies done on rat pancreatic cells and rat pituitary somatotropes have also shown activin A's effect of increasing intracellular calcium levels [53, 54]. However, these studies were conducted in functionally different cell types than the vascular smooth muscle cells that were used for our studies which could explain why we observed activin A calcium-augmenting effects only in the presence of KCl. When SHR cells were directly stimulated with activin A, there was no increased signal, which suggests that Activin A by itself does not induce calcium entry (Figure 17). Since the time period of our direct activin A stimulation calcium assays were approximately 2 minutes, we wanted to see if extending the imaging period upon direct activin A stimulation to 15 minutes would enhance calcium influx over time (Figure 14). The results showcased no rise in intracellular calcium levels upon activin A stimulation over the 15-minute imaging period. A study by Shibata et al. found that direct activin A stimulation elevated intracellular calcium levels in rat islet cells over a time-span of approximately 10 minutes which is why we decided to examine the effects of direct activin A application through our Fluo-4 studies over a 15-minute time period [55]. Overall, our activin A effects in mediating calcium entry in SHR cells mainly consist of augmentation of a KCl-induced response. This could potentially be explained by a post-translational modification of the LTCC by activin A. A study by Li et al. has shown that protein kinase A (PKA), through phosphorylation of the α1c subunit of the Cav1.2, increases channel activity and therefore enhances calcium influx [56]. Another study looking at activin signalling in granulosa cells has shown that PKA inhibitors abolished activin A-dependent Smad2 expression, which highlights a potential relationship between PKA and activin A signalling that could be applicable in our studies [57].

Furthermore, the use of the LTCC agonist, BayK 8644 (10^{-6} M), elicited contraction in SHR vessels as shown in Figure 4. However, there was variability in BayK (10^{-6} M) inducing vessel contraction even when vessels were tested for viability with KCl (125 mM) prior to experimentation. Due to this variability and the need for challenging vessels with KCl, washing then applying BayK 8644, FST was not used in these particular studies. We wanted to then take another approach with BayK 8644 by first priming both control SHR and FST-treated vessels with 30 mM KCl prior to challenging with BayK (10^{-6} M). A recent paper by Haam et al. also previously stated difficulty in obtaining stable contraction in rat mesenteric vessels with the BayK 8644 compound [58]. However, upon priming vessels with 15 mM of KCl , they were able to obtain contraction with BayK 8644, but it was not stated how long this priming period took place. Activating LTCCs with KCl would make it more feasible for BayK 8644 to shift the voltage sensitivity of these channels and augment contraction. Although our FST vessels showed a reduction in contractile response with BayK 8644, the compound did not augment the contraction caused by KCl in control vessels. A study by Aokia et al. tested the effects of BayK 8644 on dog cerebral, coronary and mesenteric arteries and also found that BayK was not effective in producing contraction in mesenteric arteries [59]. We then tested another LTCC agonist, FPL 64176, and as shown in Figure 5, although FPL 64176 (10^{-5} M) elicited contraction in WKY and SHR vessels, short-term FST treatment was not able to lower this contraction. Since FPL 64176 modifies pore properties of the LTCC, it could be that FST is acting on LTCCs to reduce KCl contraction but is not able to restore the pore alterations caused by FPL 64176 [60]. A study conducted by Fan et al. has demonstrated that FPL 64176 altered pore arrangements of the LTCC in rat ventricular myocytes and rendered the channel permeant to ions other than calcium that typically act as channel blocker such as cadmium [79].

Although the majority of our calcium cell assays were done with a 125 mM dose of KCl, when we challenged SHR cells with a more physiologically relevant dose of KCl (30 mM) in an isotonic condition, FST pre-treatment of cells still had a significant effect of lowering intracellular calcium levels compared to control cells (Figure 7). A study by Cameron et al. examining calcium handling in neuronal cells using various calcium AM dyes also used a 30 mM dose of KCl to trigger a rise in intracellular calcium for their experiments [61].

Since FST is a potent inhibitor of activins, we wanted to further examine the mechanisms through which activin A augments vessel contraction and intracellular calcium levels as that could indicate the pathways that FST mediates to lower contraction [40]. As shown in Figure 12, when intracellular calcium stores were disrupted with treatment of cells with thapsigargin, activin A effects were still present. Thapsigargin is a potent inhibitor of the Ca^{2+} ATPase, acting to render ineffective the calcium transport from intracellular stores [62]. In a study done by Hasty and Harrison, administration of thapsigargin has been shown to increase blood pressure, highlighting a relationship between endoplasmic reticulum stress and HTN [80]. However, another study by Kirby et al. found that thapsigargin blocked contraction and intracellular calcium transients in cardiac cells [81]. Although our calcium assay results displayed an initial increase calcium rise with thapsigargin pre-treatment, this rise did not reach statistical significance and therefore thapsigargin did not induce an intracellular calcium transient in the SHR cells. When cells were placed in a calcium-free media, activin A effects were prevented. Therefore, it is likely that FST acts indirectly through potent neutralization of activin A, on the LTCC to hinder calcium influx from the extracellular medium. Another possibility is that FST can alter the membrane potential of the smooth muscle cell, making depolarization and subsequent calcium influx less likely by contributing to hyperpolarization of the cell.

To provide further evidence that the fluorescent signals obtained with our Fluo-4 calcium assays were not simply due to osmotic effects, in addition to the iso-tonic condition Fluo-4 set-up in Figure 7, we also ran an experiment with mannitol as an osmotic control. Mannitol induced a rise in fluorescent signal that was similar to the signal observed with dH_2O-stimulated cells (Figure 14). The rise in calcium signal obtained with KCl (125 mM) was significantly higher than mannitol and dH_2O-stimulated cells, signifying that KCl-induced rise in calcium signal, obtained with Fluo-4 is not due to osmotic effects but rather an actual effect on the vascular smooth muscle cell calcium channels or intracellular calcium stores. Mannitol is a widely used osmotic control in literature as it changes the osmotic environment, as assessed in cell studies but typically does not induce functional changes such as mediation of intracellular calcium levels [64].

Photobleaching is a phenomenon that causes a decrease in fluorescent signal over time due to repeated exposure to light. Some of our Fluo-4 assay set-ups did show a diminishing signal towards the end of the imaging period which could have been due to this photobleaching effect. When we reduced the imaging time and frequency, the magnitude of signal improved in addition to a change in the signal drop from a steep reduction to a more gradual decline and plateau (Figure 13). This improvement in signal with reduced imaging could be due to the mitigation of photobleaching by reducing exposure of the cells loaded with Fluo-4 to light. It has been reported that Fluo-4 is not as resistant to photodestruction as other fluorescent calcium indicators such as Calcium Orange, which show minimal reduction in fluorescence over time, despite constant illumination [65]. A study by Lopez et al. found an apparent decay in fluorescent intensity within 20 seconds of imaging C2C12 cells loaded with Fluo-4 [82]. Although, it is important to note that this study had a higher rate of imaging frequency (3 frames/second) than the assays conducted in our studies.

Lastly, since some of the SHR cells used for the Fluo-4 calcium assays had been later passage cells, we wanted to investigate whether the LTCC was still being expressed in these passages. As shown in Figure 8, SHR passage 38-39 cells pre-treated with nifedipine showed a significant lowering of calcium signal, indicating the presence of the LTCC, for which nifedipine is an effective and selective blocker [66]. However, since other studies looking at KCl-induced calcium rise through calcium imaging assays, specifically in rat vascular smooth muscle cells, used earlier passages (P3-10), we also shifted to using earlier passage cells for our most recent experiments [67]. Later cell passages of VSMCs are less typically used for experiments as they may change from a contractile state to a synthetic phenotype with passage number, which could affect the contractile machinery present in the cells [68, 69]. The contractile phenotype in comparison to the synthetic one has a decreased cell size and an elongated, spindle shape [70]. All of our cells prior to use for Fluo-4 calcium assays were routinely monitored for any morphological changes that would indicate a synthetic phenotype.

To examine the effects of short-term FST treatment of SHR vascular smooth muscle on intracellular potassium, IPG-1 fluorescent potassium assays were carried out (Figure 18). Cells pre-treated with activin A displayed no changes in intracellular potassium levels upon KCl challenge (125 mM) compared to control cells challenged with KCl (Figure 19). This suggests that activin A does not augment KCl-induced intracellular potassium entry as it does calcium entry. We also showed that direct activin A stimulation does not induce potassium influx as there was no steady increase in signal with activin A challenge compared to cells challenged with Activin A buffer (Figure 17). This result is in line with our Fluo-4 calcium studies as we have not shown any calcium rise with direct activin A stimulation either. However, Mogami et al. have shown that in HIT-T15 cells, when activin A was added to a patch-clamping bath solution, the

opening of K-ATP channels were prevented [46]. Outward K-ATP currents were inhibited in these cells upon activin A addition and eventually restored upon activin A removal [46]. Closing of K-ATP channels typically results in reduced potassium efflux and thereby, an increase in intracellular potassium levels [71]. The inconsistency in results from our assays and Mogami's patch clamping experiments could be explained due to variability in the results obtained from the IPG-1 cell assay and patch-clamping technique that could more directly measure K-ATP channel activity [46]. Additionally, functional differences between SHR VSMCs and the HIT-T15 insulinoma cells used in the paper could be another reason that different cell types have distinct modes of potassium handling [46].

Additionally, we wanted to assess membrane potential changes in SHR cells with FST treatment. When cells were pre-treated with FST and then challenged with KCl, there was a significant drop in signal, indicating a less depolarized state of the cells (Figure 22). Therefore, although FST doesn't change membrane potential directly, it could be playing a secondary role in reducing depolarization in response to KCl through the modulation of K-ATP activity. K-ATP channels are important regulators of membrane potential in vascular smooth muscle as their closing induces depolarization while their opening causes membrane hyperpolarization, a phenomenon which FST may regulate [49]. Furthermore, an issue that we ran into during the completion of our $DiBAC_4(3)$ assays was a diminishing signal over time, similarly to what occurred with some of the previous Fluo-4 studies. To mitigate reduction in signal, we examined whether the $DiBAC_4(3)$ dye was subject to photobleaching with our experiment set-up which was imaging at 2 frame/second (Figure 23). When imaging was paused for a duration of 3-4 minutes, the reduction in constant exposure to light seemed to recover the signal in both control and FST pre-treated cells (Figure 23). However, when looking at the morphology of cells before and after

120 seconds of continual imaging, there were no visibly distinct changes in their shape or fluorescence. A study using the $DiBAC_4(3)$ dye for imaging of guard cell protoplasts superfused their cells on a constant basis with the dye to prevent photobleaching [72]. For our studies, cutting down on the total imaging time and imaging frequency was sufficient in helping maintain the signal and preventing its decay over time, as shown in Figure 22.

Furthermore, we have also shown that FST effects are not generalizable to angiotensin II, as short-term FST treatment was not able to reduce contraction caused by 10^{-7} M angiotensin II (Figure 9). However, it is important to note that the contraction obtained with angiotensin II even in control vessels was not very stable. Angiotensin II type 2 receptor is prone to tachyphylaxis which prevented us from conducting dose response experiments on the same vessel, similar to what was done for phenylephrine and 5-HT [83]. A study by Kuttan and Sim have found that SHR vessels are prone to tachyphylaxis and that's associated with a decrease in affinity of angiotensin II for the receptor as well changes induced in the coupling efficiency of the agonist-receptor system [84]. Contractility studies conducted with phenylephrine and 5-HT showed that FST effects in reducing contraction could be extended to these other agonists (Figure 10, 11). Additionally, we determined that activin A neutralization, as opposed to activin B, had a similar contraction-lowering effect to FST vessels with both phenylephrine and 5-HT. This finding suggests that FST is exerting its effects on lowering receptor-mediated contraction through activin A mediation.

Lastly, immunohistochemistry studies staining for pSMAD3 have revealed increased pSMAD3 expression in SHR control vessels that was lowered with short-term FST treatment. This further supports that FST effects are largely mediated through neutralization of activin signalling. Additionally, since SHR control vessels had a significantly higher nuclear pSMAD3

staining than WKY control vessels, this suggests that the hypercontractile phenotype stated in literature to be present in SHR vessels as opposed to normotensive WKY vessels is associated with increased activin signalling [73]. Additionally, immunohistochemistry staining for p-MYPT was carried out and results showed a more prominent significant increase in p-MYPT levels in the medial layer of SHR vessels pre-treated with KCl over other agonists such as angiotensin II and activin A (Figure 27). Consistent with these results, relevant literature has shown that both KCl and angiotensin II short-term treatment have been found to increase phosphorylation of MYPT1 in rat renal arteries and vascular smooth muscle cells, respectively [74, 75].

In conclusion, this study has highlighted that FST lowers potassium-induced contraction in HTN through activin A neutralization. The mechanism through which FST exerts its contraction-lowering effects likely include the blocking of calcium entry in VSMCs as FST acts similarly in mediating calcium influx to a known blocker of the LTCC, nifedipine. Additionally, FST lowers intracellular potassium, and it could be doing this by reducing potassium entry or enhancing potassium leak, upon KCl stimulation. Future research needs to assess the exact functional relationship between FST and potassium channels prominent in VSMCs, such as K-ATP.

Future Directions

Our next steps include the carrying out of both immunohistochemistry and immunofluorescence studies staining for p-MYPT on cells. We want to examine whether short-term FST treatment (500 ng/ml) can lower p-MYPT levels that are elevated in SHR vessels stimulated with KCl (125 mM for 5 minutes). This would signify a potential role of FST in reducing Rho/ROCK contractile pathway activity that is enhanced with KCl stimulation. We are also in the midst of completing Fura-2 experiments to determine if direct activin A stimulation, independent of KCl, would affect intracellular calcium levels, as our Fluo-4 studies did not show this. Fura-2 may be useful for direct activin A stimulation experiments as it is a ratiometric dye that can measure calcium levels with potentially greater sensitivity than Fluo-4. Additionally, the fura-2 indicator is resistant to concerns associated with diminishing signal due to photobleaching over time. Lastly, we want to determine if activin A effects in augmenting intracellular calcium levels involves PKA signalling. To do this, we are using a PKA inhibitor (KT 5720) in our Fluo-4 studies and may use a PKA activity-sensing assay to more directly assess whether activin A signalling involves PKA.

Future directions for our contractility experiments can include testing potassium channel activators, such as the Kv7 channel agonist, retigabine, to see if FST effects are similar to the vasorelaxation induced by retigabine. Additionally, pharmacological agents that induce opening of the K-ATP channel such as cromakalim will be used to examine if FST is able to similarly cause vessel relaxation in vessels that are pre-treated with K-ATP channel blocker, glibenclamide.

Works Cited

[1] Pickersgill, S. J., Msemburi, W. T., Cobb, L., Ide, N., Moran, A. E., Su, Y., ... & Watkins, D. A. (2022). Modeling global 80-80-80 blood pressure targets and cardiovascular outcomes. *Nature Medicine*, *28*(8), 1693-1699.

[2] Coronado, F., Melvin, S. C., Bell, R. A., & Zhao, G. (2022). Peer Reviewed: Global Responses to Prevent, Manage, and Control Cardiovascular Diseases. *Preventing Chronic Disease*, *19*.

[3] Huang, X., Lee, K., Wang, M. C., Shah, N. S., & Khan, S. S. (2022). Age at Diagnosis of Hypertension by Race and Ethnicity in the US From 2011 to 2020. *JAMA cardiology*, *7*(9), 986-987.

[4] Kaufman, J. J., MAXWELL, M. H., CRAVEN, J. D., & OKUN, R. (1971). Hypertension—primary and secondary. *Annals of Internal Medicine*, *75*(5), 761-776.

[5] Carretero, O. A., & Oparil, S. (2000). Essential hypertension: part I: definition and etiology. *Circulation*, *101*(3), 329-335.

[6] Onusko, E. (2003). Diagnosing secondary hypertension. *American Family Physician*, *67*(1), 67-74.

[7] Akpunonu, B. E., Mulrow, P. J., & Hoffman, E. A. (1996). Secondary hypertension: evaluation and treatment. *Disease-a-Month*, *42*(10), 609-722.

[8] Messerli, F. H., Williams, B., & Ritz, E. (2007). Essential hypertension. *The Lancet*, *370*(9587), 591-603.

[9] GIFFORD Jr, R. W., & TARAZI, R. C. (1978). Resistant hypertension: diagnosis and management. *Annals of Internal Medicine*, *88*(5), 661-665.

[10] Badyal, D. K., Lata, H., & Dadhich, A. P. (2003). Animal models of hypertension and effect of drugs. *Indian Journal of Pharmacology*, *35*(6), 349-362.

[11] Doggrell, S. A., & Brown, L. (1998). Rat models of hypertension, cardiac hypertrophy and failure. *Cardiovascular Research*, *39*(1), 89-105.

[12] Mohammed-Ali, Z., Carlisle, R. E., Nademi, S., & Dickhout, J. G. (2017). Animal models of kidney disease. In *Animal Models for the Study of Human Disease* (pp. 379-417). Academic Press.

[13] Reckelhoff, J. F., Cardozo, L. L. Y., & Fortepiani, M. L. A. (2018). Models of hypertension in aging. In *Conn's Handbook of Models for Human Aging* (pp. 703-720). Academic Press.

[14] Milsted, A., Marcelo, M. C., Turner, M. E., & Ely, D. L. (1998). Female Wistar–Kyoto and SHR/y rats have the same genotype but different patterns of expression of renin and angiotensinogen genes. *Journal of hypertension*, *16*(6), 823-828.

[15] Beevers, G., Lip, G. Y., & O'Brien, E. (2001). The pathophysiology of hypertension. *BMJ*, *322*(7291), 912-916.

[16] Bridges, L. E., Williams, C. L., Pointer, M. A., & Awumey, E. M. (2011). Mesenteric artery contraction and relaxation studies using automated wire myography. *JoVE (Journal of Visualized Experiments)*, (55), e3119.

[17] Endemann, D. H., & Schiffrin, E. L. (2004). Endothelial dysfunction. *Journal of the American Society of Nephrology*, *15*(8), 1983-1992.

[18] Cahill, P. A., Redmond, E. M., & Sitzmann, J. V. (2001). Endothelial dysfunction in cirrhosis and portal hypertension. *Pharmacology & Therapeutics*, *89*(3), 273-293.

[19] Zhu, J., Angelov, S., Alp Yildirim, I., Wei, H., Hu, J. H., Majesky, M. W., ... & Dichek, D. A. (2021). Loss of transforming growth factor beta signaling in aortic smooth muscle cells causes endothelial dysfunction and aortic hypercontractility. *Arteriosclerosis, Thrombosis, and Vascular Biology*, *41*(6), 1956-1971.

[20] Rodrigo, R., González, J., & Paoletto, F. (2011). The role of oxidative stress in the pathophysiology of hypertension. *Hypertension Research*, *34*(4), 431-440.

[21] Kuo, I. Y., & Ehrlich, B. E. (2015). Signaling in muscle contraction. *Cold Spring Harbor Perspectives in Biology*, *7*(2), a006023.

[22] Ivey, M. E., Osman, N., & Little, P. J. (2008). Endothelin-1 signalling in vascular smooth muscle: pathways controlling cellular functions associated with atherosclerosis. *Atherosclerosis*, *199*(2), 237-247.

[23] Janssen, L. J., Tazzeo, T., Zuo, J., Pertens, E., & Keshavjee, S. (2004). KCl evokes contraction of airway smooth muscle via activation of RhoA and Rho-kinase. *American Journal of Physiology-Lung Cellular and Molecular Physiology*, *287*(4), L852-L858.

[24] Sakurada, S., Takuwa, N., Sugimoto, N., Wang, Y., Seto, M., Sasaki, Y., & Takuwa, Y. (2003). Ca^{2+}-dependent activation of Rho and Rho kinase in membrane depolarization–induced and receptor stimulation–induced vascular smooth muscle contraction. *Circulation Research*, *93*(6), 548-556.

[25] Somlyo, A. P., & Somlyo, A. V. (2003). Ca^{2+} sensitivity of smooth muscle and nonmuscle myosin II: modulated by G proteins, kinases, and myosin phosphatase. *Physiological Reviews*, *83*(4), 1325-1358.

[26] Rattan, S., Phillips, B. R., & Maxwell, P. J. (2010). RhoA/Rho-kinase: pathophysiologic and therapeutic implications in gastrointestinal smooth muscle tone and relaxation. *Gastroenterology*, *138*(1), 13-18.

[27] Suzuki, N., Hajicek, N., & Kozasa, T. (2009). Regulation and physiological functions of G12/13-mediated signaling pathways. *Neurosignals*, *17*(1), 55-70.

[28] Seccia, T. M., Rigato, M., Ravarotto, V., & Calò, L. A. (2020). ROCK (RhoA/Rho kinase) in cardiovascular–renal pathophysiology: a review of new advancements. *Journal of Clinical Medicine*, *9*(5), 1328.

[29] Wynne, B. M., Chiao, C. W., & Webb, R. C. (2009). Vascular smooth muscle cell signaling mechanisms for contraction to angiotensin II and endothelin-1. *Journal of the American Society of Hypertension*, *3*(2), 84-95.

[30] Fukata, Y., Kaibuchi, K., & Amano, M. (2001). Rho–Rho-kinase pathway in smooth muscle contraction and cytoskeletal reorganization of non-muscle cells. *Trends in Pharmacological Sciences*, *22*(1), 32-39.

[31] Touyz, R. M., Alves-Lopes, R., Rios, F. J., Camargo, L. L., Anagnostopoulou, A., Arner, A., & Montezano, A. C. (2018). Vascular smooth muscle contraction in hypertension. *Cardiovascular Research*, *114*(4), 529-539.

[32] Puetz, S., Lubomirov, L. T., & Pfitzer, G. (2009). Regulation of smooth muscle contraction by small GTPases. *Physiology*, *24*(6), 342-356.

[33] Moosmang, S., Schulla, V., Welling, A., Feil, R., Feil, S., Wegener, J. W., ... & Klugbauer, N. (2003). Dominant role of smooth muscle L-type calcium channel Cav1. 2 for blood pressure regulation. *The EMBO Journal*, *22*(22), 6027-6034.

[34] Kuo, I. Y., & Ehrlich, B. E. (2015). Signaling in muscle contraction. *Cold Spring Harbor Perspectives in Biology*, *7*(2), a006023.

[35] Jackson, W. F. (2017). Potassium channels in regulation of vascular smooth muscle contraction and growth. *Advances in Pharmacology*, *78*, 89-144.

[36] Dart, C. (2014). Verdict in the Smooth Muscle KATP Channel Case: Guilty of Blood Pressure Control But Innocent of Sudden Death Phenotype. *Hypertension*, *64*(3), 457-458.

[37] Sobey, C. G. (2001). Potassium channel function in vascular disease. *Arteriosclerosis, Thrombosis, and Vascular Biology*, *21*(1), 28-38.

[38] Namwanje, M., & Brown, C. W. (2016). Activins and inhibins: roles in development, physiology, and disease. *Cold Spring Harbor Perspectives in Biology*, *8*(7), a021881.

[39] Chen, Y. G., Wang, Q., Lin, S. L., Chang, C. D., Chung, J., & Ying, S. Y. (2006). Activin signaling and its role in regulation of cell proliferation, apoptosis, and carcinogenesis. *Experimental Biology and Medicine*, *231*(5), 534-544.

[40] Tsuchida, K., Nakatani, M., Hitachi, K., Uezumi, A., Sunada, Y., Ageta, H., & Inokuchi, K. (2009). Activin signaling as an emerging target for therapeutic interventions. *Cell Communication and Signaling*, *7*(1), 1-11.

[41] Harrington, A. E., Morris-Triggs, S. A., Ruotolo, B. T., Robinson, C. V., Ohnuma, S. I., & Hyvönen, M. (2006). Structural basis for the inhibition of activin signalling by follistatin. *The EMBO Journal*, *25*(5), 1035-1045.

[42] Kimura, F., Sidis, Y., Bonomi, L., Xia, Y., & Schneyer, A. (2010). The follistatin-288 isoform alone is sufficient for survival but not for normal fertility in mice. *Endocrinology*, *151*(3), 1310-1319.

[43] Sidis, Y., Mukherjee, A., Keutmann, H., Delbaere, A., Sadatsuki, M., & Schneyer, A. (2006). Biological activity of follistatin isoforms and follistatin-like-3 is dependent on differential cell surface binding and specificity for activin, myostatin, and bone morphogenetic proteins. *Endocrinology*, *147*(7), 3586-3597.

[44] Tsai, Y. L., Chang, C. C., Liu, L. K., Huang, P. H., Chen, L. K., & Lin, S. J. (2018). The association between serum activin A levels and hypertension in the elderly: A cross-sectional analysis from I-Lan Longitudinal Aging Study. *American Journal of Hypertension*, *31*(3), 369-374.

[45] D'Antona, D., Reis, F. M., Benedetto, C., Evans, L. W., Groome, N. P., de Kretser, D. M., ... & Petraglia, F. (2000). Increased maternal serum activin A but not follistatin levels in pregnant women with hypertensive disorders. *Journal of Endocrinology*, *165*(1), 157-162.

[46] Mogami, H. I. D. E., Kanzaki, M., Nobusawa, R., Zhang, Y. Q., Furukawa, M., & Kojima, I. (1995). Modulation of adenosine triphosphate-sensitive potassium channel and voltage-dependent calcium channel by activin A in HIT-T15 cells. *Endocrinology*, *136*(7), 2960-2966.

[47] Kuganathan, A., Leal, M., Macdonald, M., Dickhout, J., Krepinsky, J. (2021) Follistatin as a Potential Novel Therapeutic Agent for Essential Hypertension. Poster presented at American Society of Nephrology.

[48] Fukuhara, S., Mukai, H., & Munekata, E. (1997). Activin A andAll-Trans-Retinoic Acid Cooperatively Enhanced the Functional Activity of L-type Ca^{2+} Channels in the Neuroblastoma C1300 Cell Line. *Biochemical and Biophysical Research Communications*, *241*(2), 363-368.

[49] Tinker, A., Aziz, Q., & Thomas, A. (2014). The role of ATP-sensitive potassium channels in cellular function and protection in the cardiovascular system. *British Journal of Pharmacology*, *171*(1), 12-23.

[50] Gao, M., Xue, H., Wang, Y., & Wang, H. (2005). Iptakalim, opener of KATP, reverses the enhanced expression of genes encoding KATP subunits in spontaneously hypertensive rats. *Life Sciences*, *77*(22), 2743-2751.

[51] Sonkusare, S., Palade, P. T., Marsh, J. D., Telemaque, S., Pesic, A., & Rusch, N. J. (2006). Vascular calcium channels and high blood pressure: pathophysiology and therapeutic implications. *Vascular Pharmacology*, *44*(3), 131-142.

[52] Takano, K., Yamashita, N., Kojima, I., Kitaoka, M., Teramoto, A., & Ogata, E. (1992). Effects of activin A and somatostatin on intact FSH secretion and intracellular Ca^{2+} concentration in human FSH-secreting pituitary adenoma cells. *Biochemical and Biophysical Research Communications*, *182*(3), 1408-1415.

[53] Shibata, H., Kanzaki, M., Takeuchi, T., Miyazaki, J. I., & Kojima, I. (1996). Two distinct signaling pathways activated by activin a in glucose-responsive pancreatic β-cell lines. *Journal of Molecular Endocrinology*, *16*(3), 249-258.

[54] Tasaka, K., Kasahara, K., Masumoto, N., Mizuki, J., Kurachi, H., Miyake, A., & Tanizawa, O. (1992). Activin A increases cytosolic free calcium concentration in rat pituitary somatotropes. *Biochemical and Biophysical Research Communications*, *185*(3), 974-980.

[55] Shibata, H., Yasuda, H., Sekine, N., Mine, T., Totsuka, Y., & Kojima, I. (1993). Activin A increases intracellular free calcium concentrations in rat pancreatic islets. *FEBS Letters*, *329*(1-2), 194-198.

[56] Li, Y., Yang, H., He, T., Zhang, L., & Liu, C. (2022). Post-translational modification of Cav1. 2 and its role in neurodegenerative diseases. *Frontiers in Pharmacology*, *12*, 775087.

[57] Schmierer, B., Schuster, M. K., Shkumatava, A., & Kuchler, K. (2003). Activin a signaling induces Smad2, but not Smad3, requiring protein kinase a activity in granulosa cells from the avian ovary. *Journal of Biological Chemistry*, *278*(23), 21197-21203.

[58] Haam, C. E., Byeon, S., Choi, S., Oh, E. Y., Choi, S. K., & Lee, Y. H. (2022). Vasorelaxant effect of Trachelospermi caulis extract on rat mesenteric resistance arteries. *Molecules*, *27*(16), 5300.

[59] Asano, M., Aoki, K., Suzuki, Y., & Matsuda, T. (1987). Effects of Bay k 8644 and nifedipine on isolated dog cerebral, coronary and mesenteric arteries. *Journal of Pharmacology and Experimental Therapeutics*, *243*(2), 646-656.

[60] Fan, J. S., Yuan, Y., & Palade, P. (2001). FPL-64176 modifies pore properties of L-type Ca^{2+} channels. *American Journal of Physiology-Cell Physiology*, *280*(3), C565-C572.

[61] Cameron, M., Kékesi, O., Morley, J. W., Tapson, J., Breen, P. P., Van Schaik, A., & Buskila, Y. (2016). Calcium imaging of AM dyes following prolonged incubation in acute neuronal tissue. *PLoS One*, *11*(5), e0155468.

[62] Thastrup, O. L. E., Cullen, P. J., Drøbak, B. K., Hanley, M. R., & Dawson, A. P. (1990). Thapsigargin, a tumor promoter, discharges intracellular Ca^{2+} stores by specific inhibition of the endoplasmic reticulum Ca2 (+)-ATPase. *Proceedings of the National Academy of Sciences*, *87*(7), 2466-2470.

[63] Pratt, P. F., Bonnet, S., Ludwig, L. M., Bonnet, P., & Rusch, N. J. (2002). Upregulation of L-type Ca2+ channels in mesenteric and skeletal arteries of SHR. *Hypertension*, *40*(2), 214-219.

[64] Santiago, A. R., Rosa, S. C., Santos, P. F., Cristóvao, A. J., Barber, A. J., & Ambrósio, A. F. (2006). Elevated glucose changes the expression of ionotropic glutamate receptor subunits and impairs calcium homeostasis in retinal neural cells. *Investigative Ophthalmology & Visual Science*, *47*(9), 4130-4137.

[65] Thomas, D., Tovey, S. C., Collins, T. J., Bootman, M. D., Berridge, M. J., & Lipp, P. (2000). A comparison of fluorescent Ca2+ indicator properties and their use in measuring elementary and global Ca2+ signals. *Cell calcium*, *28*(4), 213-223.

[66] Khan, K. M., Patel, J. B., & Schaefer, T. J. (2019). Nifedipine.

[67] Barbagallo, M., Shan, J., Pang, P. K., & Resnick, L. M. (1995). Effects of dehydroepiandrosterone sulfate on cellular calcium responsiveness and vascular contractility. *Hypertension*, *26*(6), 1065-1069.

[68] Chang, S., Song, S., Lee, J., Yoon, J., Park, J., Choi, S., ... & Choi, C. (2014). Phenotypic modulation of primary vascular smooth muscle cells by short-term culture on micropatterned substrate. *PloS one*, *9*(2), e88089.

[69] Sugita, S., Mizutani, E., Hozaki, M., Nakamura, M., & Matsumoto, T. (2019). Photoelasticity-based evaluation of cellular contractile force for phenotypic discrimination of vascular smooth muscle cells. *Scientific reports*, *9*(1), 3960.

[70] Rzucidlo, E. M., Martin, K. A., & Powell, R. J. (2007). Regulation of vascular smooth muscle cell differentiation. *Journal of Vascular Surgery*, *45*(6), A25-A32.

[71] Ashcroft, F. M. (2005). ATP-sensitive potassium channelopathies: focus on insulin secretion. *The Journal of Clinical Investigation*, *115*(8), 2047-2058.

[72] Konrad, K. R., & Hedrich, R. (2008). The use of voltage-sensitive dyes to monitor signal-induced changes in membrane potential–ABA triggered membrane depolarization in guard cells. *The Plant Journal*, *55*(1), 161-173.

[73] Wilson, C., Zhang, X., Buckley, C., Heathcote, H. R., Lee, M. D., & McCarron, J. G. (2019). Increased vascular contractility in hypertension results from impaired endothelial calcium signaling. *Hypertension*, *74*(5), 1200-1214.

[74] Ratz, P. H., Berg, K. M., Urban, N. H., & Miner, A. S. (2005). Regulation of smooth muscle calcium sensitivity: KCl as a calcium-sensitizing stimulus. *American Journal of Physiology-Cell Physiology*, *288*(4), C769-C783.

[75] Kirabo, A., Kearns, P. N., Jarajapu, Y. P., Sasser, J. M., Oh, S. P., Grant, M. B., ... & Sayeski, P. P. (2011). Vascular smooth muscle Jak2 mediates angiotensin II-induced hypertension via increased levels of reactive oxygen species. *Cardiovascular Research*, *91*(1), 171-179.

[76] Leung, A. A., Williams, J. V., Tran, K. C., & Padwal, R. S. (2022). Epidemiology of resistant hypertension in Canada. *Canadian Journal of Cardiology*, *38*(5), 681-687.

[77] McDonough, S. I., Mori, Y., & Bean, B. P. (2005). FPL 64176 modification of CaV1. 2 L-type calcium channels: dissociation of effects on ionic current and gating current. *Biophysical Journal*, *88*(1), 211-223.

[78] Yndestad, A., Larsen, K. O., Øie, E., Ueland, T., Smith, C., Halvorsen, B., ... & Andreassen, A. K. (2009). Elevated levels of activin A in clinical and experimental pulmonary hypertension. *Journal of Applied Physiology*, *106*(4), 1356-1364.

[79] Fan, J. S., Yuan, Y., & Palade, P. (2001). FPL-64176 modifies pore properties of L-type Ca^{2+} channels. *American Journal of Physiology-Cell Physiology*, *280*(3), C565-C572.

[80] Hasty, A. H., & Harrison, D. G. (2012). Endoplasmic reticulum stress and hypertension—a new paradigm. *The Journal of Clinical Investigation*, *122*(11), 3859-3861.

[81] Kirby, M. S., Sagara, Y., Gaa, S., Inesi, G., Lederer, W. J., & Rogers, T. B. (1992). Thapsigargin inhibits contraction and Ca^{2+} transient in cardiac cells by specific inhibition of the sarcoplasmic reticulum Ca^{2+} pump. *Journal of Biological Chemistry*, *267*(18), 12545-12551.

[82] Lopez-Ayon, G. M., Oliver, D. J., Grutter, P. H., & Komarova, S. V. (2012). Deconvolution of calcium fluorescent indicator signal from AFM cantilever reflection. *Microscopy and Microanalysis*, *18*(4), 808-815.

[83] Duarte, D. A., Parreiras-e-Silva, L. T., Oliveira, E. B., Bouvier, M., & Costa-Neto, C. M. (2022). Angiotensin II type 1 receptor tachyphylaxis is defined by agonist residence time. *Hypertension*, *79*(1), 115-125.

[84] Kuttan, S. C., & Sim, M. K. (1993). Angiotensin II-induced tachyphylaxis in aortas of normo-and hypertensive rats: changes in receptor affinity. *European Journal of Pharmacology*, *232*(2-3), 173-180.

[85] Paulis, L., Líšková, S., Pintérová, M., Dobešová, Z., Kuneš, J., & Zicha, J. (2007). Nifedipine-sensitive noradrenergic vasoconstriction is enhanced in spontaneously hypertensive rats: the influence of chronic captopril treatment. *Acta Physiologica*, *191*(4), 255-266.